ALLEGHENY COLLEGE



Birefringence in Liquid Crystal Elastomers:

A Study on the Effect of Applied Stress on LCE Birefringence

Christopher Charles Blackstone

Chemistry '11

4/15/2011

Birefringence in Liquid Crystal Elastomers: A Study on the Effect of Applied Stress on the LCE Birefringence

Christopher Charles Blackstone
Senior Comprehensive Project
Spring 2011

Submitted to the Allegheny College
Department of Chemistry
to partially fulfill the requirements for the degree of
Bachelor of Science

Committee Members:
Dr. David Statman
Dr. Alice Deckert
Dr. Ryan Van Horn

I hereby recognize and pledge to fulfill my responsibilities, as defined by the Honor Code, and to maintain the integrity of both myself and the College community as a whole.

Pledge: _____

Christopher Charles Blackstone

Acknowledgments.
Dr. Statman: Thank you for all of your help this year. I most certainly could not have completed this project without your willingness to listen to and answer thoughtfully my multitude of questions. If not for that, I would probably still have no idea what I was doing in the lab. You made an unfamiliar environment comfortable for me. Thanks also for the family environment you helped to create in the lab, as well as the delicious Hungarian dinners.

Dr. Deckert: You've been a fantastic and supportive adviser for me over the years, and I appreciated the freedom you gave me to pursue whatever absurd ambitions I chose. Thank you also for giving me my first research opportunity. It was a great experience, a ton of fun, and I learned a lot.

Paul Luchette, Kent State University: Without you, this project would have been impossible. Thank you for not only providing me with the materials I needed, but also helping me to develop the infrastructure necessary to make LCE research sustainable at Allegheny College. Additionally, thank you for the numerous correspondences that helped me learn about every little quirk of my elastomers.

Bob Caskey and brother: Thank you for making sure all of my chemistry needs were filled and for sympathizing with my position in foreign territory. You helped me tool this lab appropriately for my purposes. Thanks also to your brother, who generously and skillfully assembled the spin caster head. You have helped make elastomer research a sustainable endeavor at Allegheny College.

Neil Donovan, Meadville Vo-Tech: Thank you for building the boxes I needed for my apparatus. They have served me very well.

Rob Timlin: Thank you for letting me into the electronics lab several times every week and making sure that I had all the materials I needed when I needed them.

Dr. Willey: Thank you for all of your help in designing and acquiring materials for the spin caster apparatus. It turned out great, and for half the projected cost, no less.

The Statman Lab: I cannot possibly imagine a more fun group of people with whom to have completed my project. No matter how poorly the research was going (and that was often pretty poorly), you guys could keep the mood light. Our daily jigsaw puzzle tradition kept me sane, Marci, and Dan, your dramatic entrances always brightened up my day. Alex, your ability to find the humor in your own mistakes made every bad lab day feel a little better, and Brandi, I always appreciated how much smiling you did. Kaitlin, thanks for helping me understand what in the world was going on in the lab, and John, well, we missed you in the second semester. Sarah, Robby, and Jockers, thank you for the breath of fresh air you brought to the lab, as well as all the assistance you gave us.

Mom and Dad: I could not have even gone to this school if not for all the sacrifices you've made for me, and I certainly would not be the person I am if not for the fantastic job you did raising me. Thanks for always being there for me, inspiring me, and encouraging me. I love you both dearly. Additionally, thank you, Dad, for helping me to put the finishing touches on my boxes.

Patrick: Thank you for your sense of humor. It always keeps me going. Good luck in college next year!

The Chemistry and Physics Compers: You guys were always around and willing to empathize with me (or complain, but the difference is slight). Thank you all for going through the same things I did and for sticking together through it all.

Anna: Thank you for being a constant presence for me this year. You kept me grounded and pleasant, no matter how bad things got. Thank you for always listening and always being willing to be there for me.

The Rest of my Family and Friends: I wish I could give each of you an individual acknowledgment, but that is unrealistic, so I will just thank all of you for your support in one big blanket statement. You guys were fantastic, and really kept me going. Aunt Jean, Oreo, and the rest of my aunts and uncles, thank you all for making home a great place to come when I needed a break. Delta Tau Delta, you guys will always be my brothers. Thank you for always giving me a second home, and for all of the great things we do together. ResLife staffers, thank you for empathizing with me on all the levels the compers could not, and for giving me some great weekends to unwind after a tough week of research. Ravine, thank you for making my job easy. You guys were fantastic. And to the rest of my family and friends not listed here, thank you for all of your support and all the good times we shared.

Table of Contents

Acknowledgments ..... **i**
Table of Contents ..... **iii**
Abstract **1**
1. Introduction **2**
1.1 Liquid Crystals Definition, Description, and Research 2
1.1.a Description of Order in Nematic Liquid Crystals 3
1.1.b Free Energy in LC Systems Under the Influence of an External Field 5
1.1.c Summary of Research in Liquid Crystal Optics 6
1.2 Description of Liquid Crystal Elastomer 8
1.3 Physical Properties of LCE 9
1.3.a Classical Elasticity 10
1.3.b Effect of Strain on Order in Nematic LCE 14
1.4 Optical Properties of LCE 15
1.5 Birefringence 15
1.5.a. Classical Birefringence 15
1.5.b Birefringence in Liquid Crystals 18
2. Experimental **21**
2.1 Synthesis of LCEs 21
2.2 Finding Young's Modulus of LCEs 23
2.3 Theory of PEM 24
2.4 Measurement of Birefringence in LCEs 26
2.5 Data Analysis 28
3. Results and Discussion **31**
3.1 Progression of Setups 31
3.2 Current Methods and Speculation on Improvement 35
4. Conclusions **37**
5. Future Considerations **38**
Appendix A: Tabulation of Raw Data **A1**
Appendix B: Photographs of Lab **A11**
References **A14**

Abstract.

Liquid crystal elastomers are cross-linked polymers with elastic mechanical properties, as well as many of the optical properties of liquid crystalline systems, such as birefringence. This study deals with the birefringence of liquid crystal elastomers. Tests were performed to determine the effects of applied stresses on the birefringence of a 10% cross-linked liquid crystal elastomer. Unfortunately, these tests did not return steady, reproducible data, and thus no conclusions could be made about the system. Instead, a treatment of the errors in the tests was performed in order to guide future researchers in this field.

1. Introduction. Liquid crystal elastomers (LCEs) have been of significant interest in the fields of physical chemistry, chemical physics and material science over the past few decades because of their intriguing mechanical, thermal, and optical properties and behaviors. LCEs have great potential in the fields of optical tuning and medical research, specifically pertaining to the development of artificial muscles.[1-10] Understanding various components of these systems is therefore of significant value in the scientific community.

The purpose of this study is to analyze various optical properties of liquid crystal elastomer systems. I begin with a definition and description of LCEs, a brief treatment of studies already completed on their thermodynamic, mechanical and optical properties, and finally a brief treatment of birefringence studies in liquid crystalline (LC) systems.

1.1 Liquid Crystals, Definition, Description, and Research. In order to understand many of the properties of the LCEs presently described, we must explore liquid crystal systems independent of elastomers. The following is a brief overview of the characteristics and behaviors of liquid crystals, as well as some significant research concerning liquid crystal optics.

First, I will compare isotropy and anisotropy. Isotropy refers to physical properties being the same throughout the system. In a liquid crystal system, this means that the molecules align themselves randomly causing all the directions to be equivalent. Consequently, the system's physical properties are equivalent in all directions. Anisotropy refers to the difference of physical properties throughout the system. In liquid crystals, this means that the molecules align along some axis, causing properties to be different in different directions. For example, if the elasticity in a material is anisotropic, stretching it an equal length along one axis may require a different amount of force than along another axis.

Another word that will appear often is mesogen, which refers to a liquid crystal molecule in its anistropic state. The mesophase is the phase in which the liquid crystals are mesogenic. The nematic phase is a specific type of mesophase in which liquid crystals order along a director axis, $\hat{\boldsymbol{n}}$, but do not possess positional order. This is the state with which we will mostly be concerned throughout this study. The clearing point or clearing temperature is the temperature at which a liquid crystal system makes a transition between mesogenic and isotropic.

Liquid crystals are materials that can enter a state of matter between liquid and solid. The molecules in the system align themselves in a fashion similar to crystal lattices but are still able to flow like liquids. This makes liquid crystals particularly susceptible to the effects of mechanical, electrical, and other fields.[11-13] Primarily in this study, we will be considering their optical properties. Birefringence is of particular interest to this study, and will be discussed in section 1.5.

1.1.a. Description of Order in Nematic Liquid Crystals. Since the orientational order of nematic liquid crystals is one of the primary contributors to their unique properties, we will now model that. Since the order is defined by an average, we must consider all the individual mesogens and how they orient relative to $\hat{\boldsymbol{n}}$ in terms of the angle θ made between the long axis of the molecule and the director.

Each liquid crystal has its own orientational distribution function $f(\theta)$, which is dependent upon the individual properties of the molecule. The molecules' orientations have spherical symmetry, rotating about their axes along polar angle θ and azimuthal angle ϕ. However, since all ϕ are equivalent, we need not consider them to describe the order of the liquid crystals. Also, because of the spherical symmetry of the system, we can define $f(\theta)$ in terms of the Legendre Polynomials.[11,15]

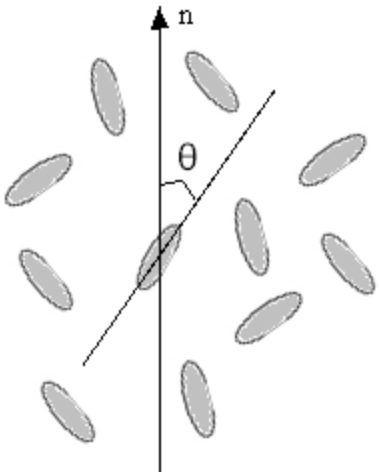

Figure 1.1. Diagram of order in a nematic liquid crystal. The director n is the average direction of the mesogens. θ is the angle between the molecular axis and the director.

$$f(\theta) = \sum_{l=0,2,4,\ldots} S_l P_l(cos\theta) \tag{1.1}$$

Only the even terms are considered because all of the odd terms sum to zero. This is due to the symmetry of the system driving S_1, S_3, S_5, etc. to 0. S is the order parameter of the system, which can be measured by various experimentations, including X-ray diffraction and birefringence measurements. It turns out that the order parameter can be approximated by the second Legendre Polynomial.[11]

$$S = S_2 = \langle P_2(cos\theta)\rangle = \langle \frac{3}{2} cos^2\theta - \frac{1}{2}\rangle \tag{1.2}$$

S will fall between 0 and 1, where 0 describe an isotropic situation (θ has values from 0 to π, with no preference to any particular angle) and 1 describes perfect order ($\theta = 0$), which is most often found in rigid crystals. For liquid crystals, S generally falls between 0.3 and 0.8.

We shall see the relationship between the order and birefringence in liquid crystals in section 1.5. For now, we will be sufficed to say that birefringence increases with increasing order. It is also important to note that liquid crystalline order is dependent on temperature. Specifically, order decreases with increasing temperature. This is consistent with intuition since

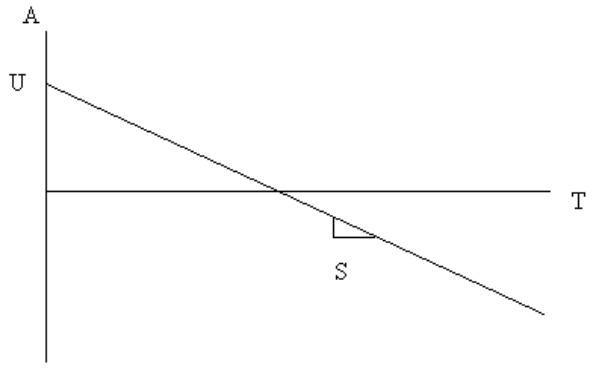

Figure 1.2. Graph of free energy as a function of temperature. The slope is defined by the change in entropy. Since the slope is negative, entropy increases with temperature, and thus order decreases, which supports proposed ideas on the behavior of liquid crystals in increasing temperatures.

higher temperatures mean the system has more energy, which in turn results in more motion, thus decreasing the system's order. Recalling thermodynamics, and specifically the free energy equation $A = U - TS$, this can also be shown. Figure 1.2 shows the graph of free energy as a function of temperature with S as the slope. Notice that the slope is negative with increasing temperature, meaning that entropy increases with temperature, and thus order decreases.

1.1.b. Free Energy of LC Systems Under the Influence of an External Field. We can look at the effect of an external field on the free energy of a liquid crystal system. The free energy of a liquid crystal is given by[14,15]

$$F_v = \int_0^L \left\{\frac{1}{2}k_1(\boldsymbol{\nabla}\times\hat{\mathbf{n}})^2 + \frac{1}{2}k_2[\hat{\mathbf{n}}\cdot(\boldsymbol{\nabla}\times\hat{\mathbf{n}})]^2 + \frac{1}{2}k_3[\hat{\mathbf{n}}\times(\boldsymbol{\nabla}\times\hat{\mathbf{n}})]^2 - \frac{1}{2}\Delta\varepsilon\varepsilon_0 E^2 cos^2(\phi-\phi')\right\}dz + W \quad (1.3)$$

F_v represents the free energy per unit volume of the liquid crystals throughout the entire system with relationship to order and the external electric field E. W represents the anchoring energy, $\Delta\varepsilon$ is the anisotropy permittivity, or the difference between the permittivities along each the axis parallel to the director and the axis perpendicular, ε_0 is the electric permittivity of free space, $\hat{\boldsymbol{n}}$ is the director, $\phi - \phi'$ describes the difference between the director angle and the direction of the electric field, and k_1, k_2 and k_3 are constants. The k_1 term describes the splay orientation of liquid

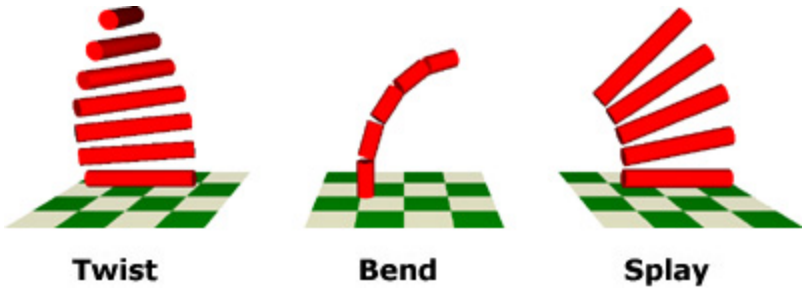

Figure 1.3. The three orientations of liquid crystals, twist, bend and splay. All three orientations are described by terms in Equation 1.3.[16]

crystals, k_2 corresponds to twist liquid crystals, and k_3 refers to bend liquid crystals. These are the three orientations that liquid crystals can take, and they are described in Figure 1.3.[14]

The system will naturally tend toward the state of lowest possible energy. We notice that there is dependence on the strength of the external field.[11,14] This makes sense since the field will influence the liquid crystals to orient in a different way, and that reorientation requires the system to work. From the condition of an applied electric field in Equation 1.3, we can infer what would happen under the condition of an applied mechanical field. If the field was in the direction of the director, the system would experience lower energy, but if the field were in some other direction, energy would increase and the liquid crystals would want to rotate toward the mechanical field direction.

1.1.c. Summary of Research in Liquid Crystal Optics. As stated above, the optical properties of liquid crystals are of great interest in materials science, physical chemistry and chemical physics. Here, we will briefly treat some of the observations made about liquid crystals, calling the reader's attention to them, but not developing the models in any great detail.

In the isotropic phase, an incident laser can cause a reorientation of liquid crystal molecules, resulting in an induced polarization. As the temperature of the system diminishes, especially approaching the clearing temperature, the optical properties of the system increase. This is expected by the same argument made when explaining the order parameter's temperature

dependence. Decreasing temperature results in less energy for the system, and thus lower molecular entropy.[11,12]

In the anisotropic state, liquid crystals tend to align their director axis along the direction of polarization of the incident light.[11,12] This is a result of the electric field inducing polarizations in the liquid crystal system. The electric field then applies a torque to the liquid crystals, causing them to rotate. Due to the system's anisotropy, the reorientation can cause a significant change in refractive index. The magnitude of the change in orientation is proportional both to the order parameter and the dielectric constant of the particular liquid crystal system.

Doping the liquid crystals with dyes has some effect on the nonlinear optics of the systems as well.[12] In the short-term, the dyes enhance the optical effects in the liquid crystals. After prolonged exposure, however, they stimulate orientation perpendicular to the polarization of the incident light instead of parallel.[11,12] The dyes absorb into the liquid crystal system under conditions of incident light and isomerize, lowering the energy of reorientation. Additionally, surface treatments of the system can cause these effects to remain even after the removal of the incident light.

The above behaviors contribute to many optical phenomena in liquid crystals. These include self-phase modulation, spatial soliton formation, passive optical switching, coherent holography and image processing, as well as various other effects.[12] Since they are not directly relevant to this study, these phenomena will not be described beyond their mention, but will simply serve as proof that liquid crystals are very optically intriguing.

1.2 Description of Liquid Crystal Elastomer. An elastomer is a cross-linked polymer system that possesses rubber-like or elastic properties.[1] A liquid crystal elastomer is simply an elastomer with mesogens incorporated either as side-chain substituents to the polymer backbone (a side-chain liquid crystal elastomer, or SCLCE), or as the monomers that comprise the backbone polymer (a main-chain liquid crystal elastomer, or MCLCE).[1,2] Figure 1.4 provides diagrams of each type.

The cross-linking of the polymer chains is what creates the elasticity of the material, but as the cross-linking density increases, the material will become more plastic, losing its flexibility. This makes intuitive sense when considering the distance between cross-linking sites on the elastomer: a lower cross-linking density means greater distance between cross-linking sites, and greater distance provides for greater freedom of movement.[1,2] When the system is able to easily

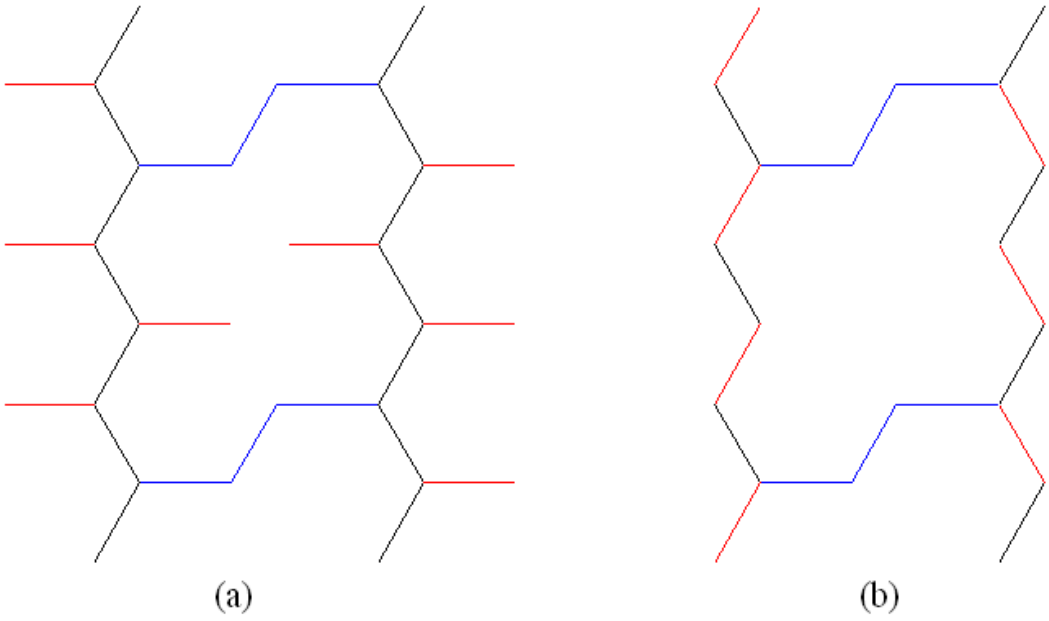

Figure 1.4. Diagrams of two different forms of LCEs: (1) is a side-chain LCE and (b) is a main-chain LCE. Liquid Crystal monomers are shown in red in both diagrams, cross-linkers are blue. In (a), the polymer backbone is shown in black. In (b), the connecting chains for the LC polymer are shown in black.

bend and stretch on the molecular level, that ability translates to macroscopic properties, allowing the material as a whole to bend and flex elastically. The opposite is true when the system is constrained.

Liquid crystal elastomers also tend to hairpin. That is to say that the chains fold over on themselves. This is characteristic of rubber materials and partially provides the elasticity of those materials. Essentially, when a mechanical force is applied to deform the elastomer, the hairpins fall out and allow the chain to straighten. Once the force is no longer incident, the system returns to its energetically favorable hairpins. These hairpins are described in Figure 1.5.

1.3 Physical Properties of LCE. The elasticity of elastomers is one of the major reasons that they are such interesting systems in material science. That elasticity is of particular interest to this study, so the mechanical properties section will be devoted primarily to elasticity in LCEs

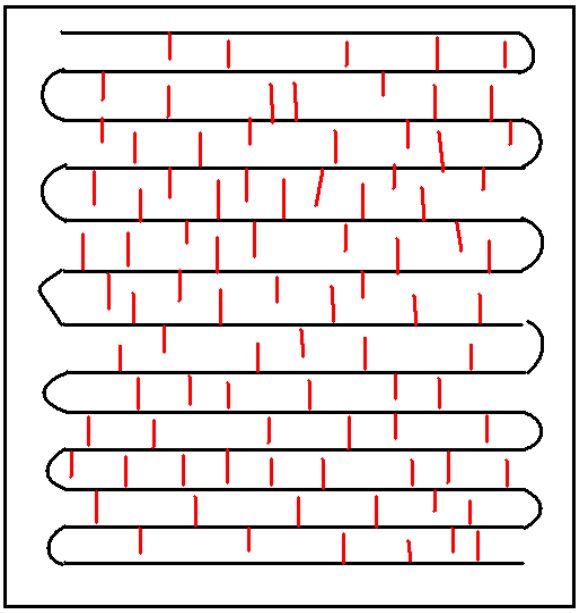

Figure 1.5. Diagram of hairpins in liquid crystal elastomers. The outer black lines are the whole elastomer, the curving black lines are the polymer chain hairpinning on itself, and the red vertical lines are the side chain liquid crystals. Notice how they are oriented in the hairpin formation, aligning themselves along the director pointing in the direction of the elastomer's long axis.

beginning with a classical model of the concept. I will then relate that model to the model for LCEs and briefly discuss the effects of temperature on the system.

1.3.a. Classical Elasticity. The basis of elasticity is the stress-strain model of material deformation. In order to stretch a material, a force must be applied along one axis. The force applied per cross-sectional area of the material is called a stress, and the stress is proportional to the amount the material is stretched, so $\frac{F}{A} \alpha \frac{\Delta l}{l}$. In order to made that proportionality an equation, we need to add a constant. For the stress-strain relationship, that constant is Young's Modulus, Y, which is a description of the elastic properties of a material. The higher the value of Y is, the less elastic the material. It makes sense to have a material-dependent constant to complete the relation because not all materials stretch the same. For example, it requires a great deal more force to stretch a steel beam than a rubber band and equal distance, even if they both have the same cross-sectional area. From all of this, we obtain the equation[14,16]

$$\frac{F}{A} = Y \frac{\Delta l}{l} \tag{1.4}$$

In Equation 1.4, $\frac{F}{A}$ gives the stress and $\frac{\Delta l}{l}$ represents the strain.

When a material is stretched in one direction without applying any force to the other surfaces, the unaffected sides will contract to accommodate the stretch and preserve the volume. This event is described by the following expression:[16]

$$\frac{\Delta w}{w} = \frac{\Delta h}{h} = -\sigma \frac{\Delta l}{l} \tag{1.5}$$

where w and h represent the width and height of the material, respectively, and σ is Poisson's ratio, another elastic property of the material that is always between 0 and ½. Notice that the sign of the length term is negative whereas the signs of the width and height terms are positive. This expresses that in the case of a stretching along l, w and h will decrease, and vice versa.

In the case of an isotropic material, *Y* and σ are the only elastic constants, as all directions are equivalent.[16] In fact, we can say σ =½ for an isotropic material by looking at Equation 1.5 in relationship to the conservation of volume we have described.

$$\Delta V = 0 = \frac{\Delta w}{w} + \frac{\Delta h}{h} + \frac{\Delta l}{l} \Rightarrow \frac{\Delta w}{w} + \frac{\Delta h}{h} = -\frac{\Delta l}{l} \Rightarrow 2\frac{\Delta w}{w} = -\frac{\Delta l}{l} \Rightarrow \frac{\Delta w}{w} = -\frac{1}{2}\frac{\Delta l}{l}$$

We can make the arguments above because of the equivalence of directions in an isotropic material. Looking at the final expression in terms of Equation 1.5, we can see that for an isotropic material, σ =½.

However, in an anisotropic material, there may be several elastic constants to account for the lack of uniformity across all directions. Consider a material with length *l* bound at one end and a particle some distance *x* from that end inside the material, as described in Figure 6. We then apply a force to the unbound end to stretch it a length Δ*l*. The particle will shift in the direction of the stress. It is immediately obvious that the displacement of the particle is proportional to the strain, since the more the material is stretched, the more the particle must intuitively move, but there is also a dependence on the distance *x* from the bound end. Specifically, the displacement is directly proportional to *x*. This is less obvious, but can still be explained intuitively by considering the extreme ends of the material. If the particle is on the bound end, or *x* = 0, then it will not move at all with the applied stress, since it is bound. However, if it is on the opposite end, at *x* = *l*, the particle will move the full distance of the stress. From this, we find the following expression:[16]

$$u_x = e_{xx}x \tag{1.6}$$

where $e_{xx} = \frac{\Delta l}{l}$ and u_x is the displacement of the particle.

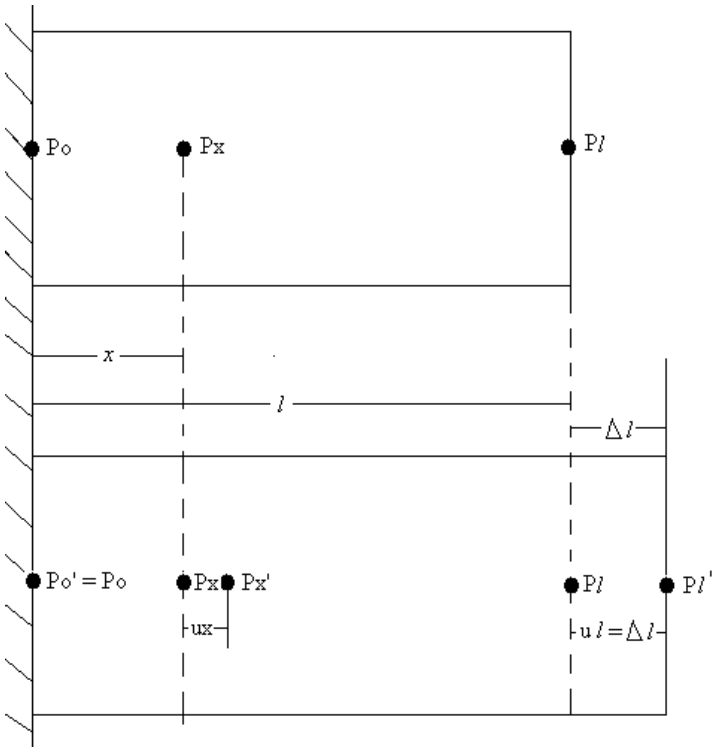

Figure 1.6. Model of the stretching of a bound material. This demonstrates the *x*-dependence of the value u_x. Notice that P_0 does not move, P_x moves somewhat, and P_l moves the entire strain Δl.

Now we will generalize the model. Since there are more dimensions, we must define the proportionality constant e_{xx} in terms of changes in u_x, and the same is true for the *y* and *z* dimensions.[16]

$$e_{xx} = \frac{\partial u_x}{\partial x},\ e_{yy} = \frac{\partial u_y}{\partial y},\ e_{zz} = \frac{\partial u_z}{\partial z} \tag{1.7}$$

In a three-dimensional model, however, the strain felt along each axis is not limited strictly to the stress on that axis. It depends also on the other axes, so we must define terms e_{xy}, e_{yx}, etc. to account for this. In order to describe these we must determine a model that accounts for the symmetry of the system while causing all non-stress rotations of the material to produce no strain. As a result, we obtain:[16]

$$e_{ij} = \frac{1}{2}\left(\frac{\partial u_j}{\partial x_i} + \frac{\partial u_i}{\partial x_j}\right),\ i,j = 1,2,3 \tag{1.8}$$

where u_1, u_2, and u_3 refer to u_x, u_y, *and* u_z, respectively and x_1, x_2, and x_3 refer to x, y, and z, respectively. Because of symmetry, the strain tensor described by this model contains six terms.

Now having the strain tensor, we may describe the tensor of elasticity, which allows us to relate the stress and strain at any point in a material. The tensor model is analogous to the model in Equation 1.4, but expanded to account for all dimensions. In order to account for the influences in various directions, we must describe the stress, S_{ij}, as a summation.[16]

$$S_{ij} = \sum_{k,l} C_{ijkl} e_{kl}\,, \quad i,j,k,l = 1,2,3 \tag{1.9}$$

Here the elastic coefficient is the fourth rank tensor C_{ijkl}. The indices i, j, k, and l describe the four ranks of the elasticity tensor. Depending on the symmetry and homogeneity of the system, it can assume up to 36 terms. These 36 terms describe how deformations along unstressed axes occur to account for the deformations in the stressed axis. We can relate C_{ijkl} to the Young's Modulus described earlier. Young's modulus deals with the stress required to stretch a material a certain length, and it is a strictly linear term that is sufficient to discuss the nature of the material, but not to describe what is happening physically inside it. Since the material does not simply stretch, but must contract in other directions, the elasticity tensor must be an extensive description of all deformations. For example, if you stretch a rubber band, you will notice that it contracts toward the center in the directions not being stretched, appearing concave. The parameters of the rubber that allow for this deformation are described by the elasticity tensor. This provides a general and comprehensive model for elasticity.

In rubber and elastomer systems, the stretch results in the extension of the long chains. Before a stress is applied, the polymers take a random orientation. As an increasing stress is applied, the polymers align themselves increasingly more linearly. This results in an entropic penalty.

1.3.b. Effect of Strain on Order in Nematic LCEs. As will be demonstrated, the stretching of an elastomer along its director axis can result in the mesogens being held in their orientation even against incident light. Interestingly, when a strain occurs perpendicular to the director up to 10%, the director does not change.[1] Above 10%, however, the director does begin to shift in the direction of the strain.

When an elastomer is stretched, the hairpins described in Figure 1.5 uncoil, causing the side chain liquid crystals to splay, the condition described by the k_1 term in Equation 1.3, as described in Figure 1.7. This could either increase the order by pushing more of the liquid crystals into a standard orientation or decrease it by pulling some liquid crystals away from the

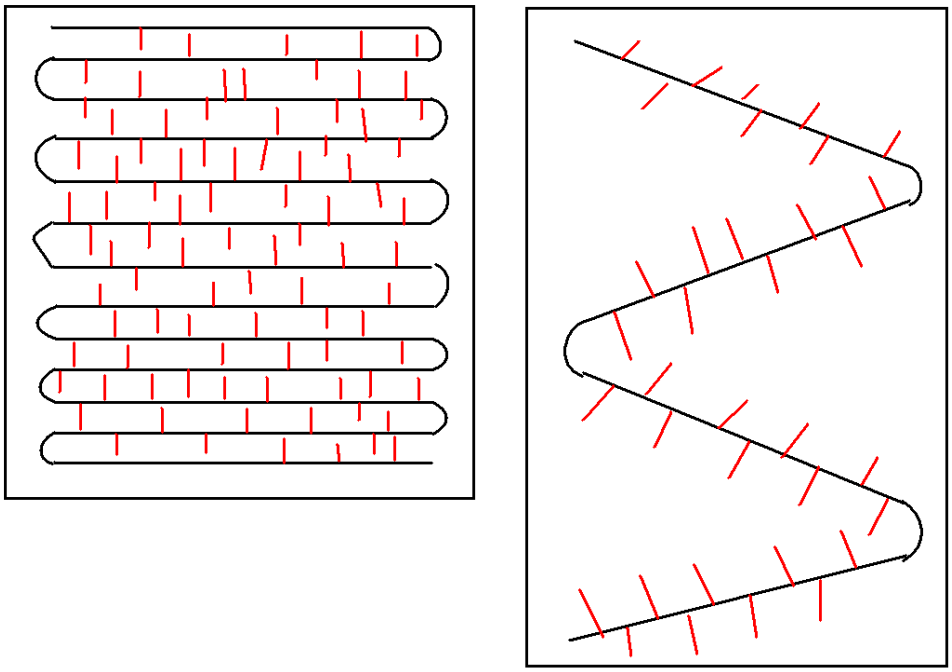

Figure 1.7. Uncoiling of the hairpins in a liquid crystal elastomer as the result of an applied stress. Notice how the liquid crystals splay upon stretching. The effects of this on birefringence are of particular interest to us.

director. The nature of that relationship is the focus of this study.

1.4 Optical Properties of LCE. Due to the liquid crystals in them, LCEs exhibit interesting optical behaviors. One of the most interesting facets of LCE optics is the ability of azobeneze-doped LCEs to transform optical energy into mechanical energy. Specifically, an LCE irradiated with blue light bends. When pretreated with UV radiation, the bend starts very slightly toward the laser source, but quickly reverses direction and bends away from it. Without the UV pretreatment, the elastomer initially bends away from the laser, but then bends back toward it. The polarization of the light relative to the long axis of the cantilever dictates the extent of the bend, with parallel orientation providing a large back-bend and perpendicularly polarized light producing a much slighter bend. [3,4]

Allowing the elastomer to float on water and then irradiating it produces a "swimming" phenomenon. The optically-induced mechanical deformations described above cause the elastomer to bend at the point of the incidence of the light, displacing water. Because the water is displaced, the elastomer moves and a new point is deformed. This causes the elastomer to move similarly to a stingray, gliding across the surface of the water. This process continues until the elastomer is no longer under the irradiation.[5]

1.5 Birefringence. Birefringence is defined as the separation of a ray of light into two perpendicularly-polarized parallel rays.[18,19] It is the consequence of a material having two refractive indices in different directions. A classical model of birefringence is presented first, followed by a model of birefringence as observed specifically in liquid crystals.

<u>1.5.a. Classical Birefringence.</u> In an anisotropic crystal lattice, differences in binding energies in different directions within the lattice cause birefringence. Essentially, if we orient a lattice such that one refractive index falls on the x-axis, n_x, and the other along the y-axis, n_y, the interactions

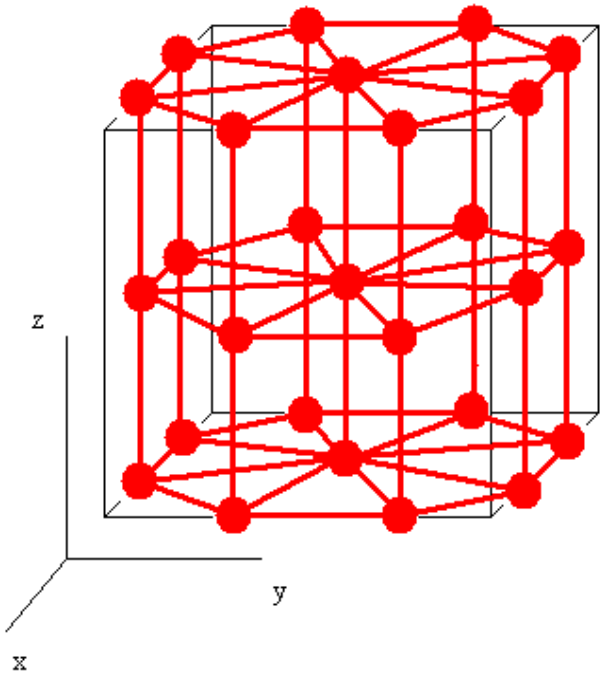

Figure 1.8. A simple hexagonal lattice is anisotropic because the bonds are not equivalent along all axes. Here, looking along the x- and y-axis are equivalent, appearing cubic, whereas looking down the z-axis appears hexagonal. Consequently, a crystal with this or another anisotropic lattice is birefringent.

of the material with light passing through will cause the x-oriented waves, E_x, and the y-oriented waves, E_y, to be out of phase. That is to say E_x and E_y will propagate with different velocities, v_x and v_y, respectively.[18] A material that behaves in this fashion is called uniaxial because it has one axis different from the other two.

Approaching this from the very smallest level can offer some explanation as to why this phenomenon occurs. When light passes through a material, it interacts with the electrons in that material. This is why the bond energies are so important to determining the refractive index along each axis. In a liquid or a gas, the molecules are free to translate, oscillate, and rotate essentially randomly. As a result, the bond energies along each axis are, on average, equivalent. However, in a crystal, the molecules are bound to a specific position and orientation, so the electron interactions may or may not be uniform on average along each axis. Unless the

structure is symmetric along all axes, as in NaCl, the electrons will behave differently along different axes of the material. The more the electrons along a given axis interact with the light oriented in that axis, the slower the light will propagate.[18] Thus, the more chemical bonds there are on a given axis (and therefore the more electrons are bound to that axis), the slower the light will propagate through the axis.

Using this conclusion, we can relate the bound electron density to the refractive index, and thus relate the birefringence to the refractive indices along each axis. Given that[18,19]

$$n=\frac{c}{v} \tag{1.10}$$

where c is the speed of light in a vacuum and v is the speed of the light after refraction, we can see that the refractive index is inversely proportional to the speed at which the light propagates through the material. Combining this with the fact that velocity decreases with increasing bound electron density, the refractive index along a given axis of a material is proportional to the bound electron density along that axis.

The birefringence itself, Δn, is given by the difference of the two refractive indices. Instead of using x and y, it is conventional to use parallel and perpendicular refractive indices. Thus we have[18]

$$\Delta n = \left|n_{\parallel} - n_{\perp}\right|. \tag{1.11}$$

If $\Delta n > 0$, then the material is birefringent.

As previously stated, birefringence causes a phase shift in the incident light. The difference in the two phases, $\Delta\phi$, is given by[18]

$$\Delta\phi = \left(\frac{2\pi}{\lambda_0}\right)\left|n_{\parallel} - n_{\perp}\right| d \tag{1.12}$$

where λ_0 is the wavelength of the light in a vacuum and d is the thickness of the material.

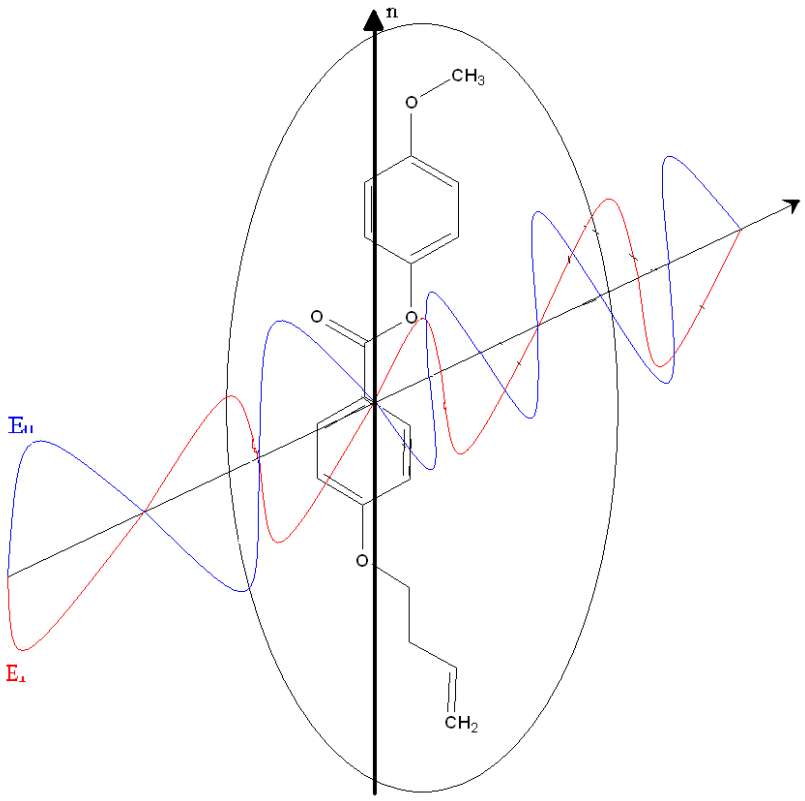

Figure 1.9. Diagram of the birefringence of a liquid crystal, 4-methoxyphenyl 4-(but-3-enyloxy)benzoate , which will be used in this study. The bond density along the director is significantly higher than perpendicular to it, giving the parallel axis a greater refractive index. This is represented by the wavelength of $E_{\parallel}$ being reduced more than the wavelength of $E_{\perp}$. Since both frequencies remain the same, this discrepancy in wavelength shows that the $E_{\parallel}$ waves are moving more slowly after passing through the liquid crystal than the $E_{\perp}$ waves.

1.5.b. Birefringence in Liquid Crystals. The actual concept of birefringence is essentially the same in liquid crystals as it is in lattice systems by definition, but here I treat birefringence as it applies specifically to liquid crystal systems.

Like in anisotropic crystal lattices, liquid crystals have two different refractive indices along two axes causing the birefringence.[11,12] We expect this because of the order with which the liquid crystals align. In nematic systems specifically, the crystals orient along a linear director axis. Just viewing the system in Figure 1.9, it becomes immediately obvious that not all

directions are physically equivalent. From that, we can infer that different axes possess different indices of refraction, and therefore the system is birefringent.

Since nearly all liquid crystals are non-magnetic, those indices of refraction are determined by the relative permittivity or dielectric constant by[11]

$$n = \sqrt{\varepsilon_r}. \tag{1.13}$$

As stated above, not all directions are equivalent in anisotropic liquid crystals, and the relative permittivity is not equivalent either. There are separate permittivities in the directions parallel and perpendicular to the director axis, respectively. Consequently, the refractive indices are different parallel and perpendicular to the director, and thus the compound is birefringent.

The difference in refractive indices can also be explained in terms of bond energies along each the parallel and perpendicular axis. Whichever axis possesses higher bond energies will have a higher refractive index. If the parallel axis has a greater refractive index, the birefringence will be positive, and if the perpendicular axis does, then birefringence will be negative.

Experimentally, it has been shown that the gap between the refractive indices closes with increasing temperature.[11] This is a result of the increasing isotropy with higher temperature. At the clearing temperature, the refractive indices immediately become equal, since there is no longer a director axis and all the directions in the liquid crystal have become equivalent. Therefore, there is a direct proportionality between the order parameter of a liquid crystal and the birefringence.

Since liquid crystals have been experimentally determined to be birefringent, we expect the same to be true of LCEs. The following experiments have been designed to determine the birefringence in LCEs as it relates to stress applied to the system, beginning with the synthesis of

these compounds, then the measurement of the Young's Modulus, the theory of the instrumentation, data collection, and data analysis.

2. Experimental. A study has been designed to find relationships between the birefringence in LCEs with varying stresses applied to the system. Those processes are outlined below.

2.1 Synthesis of LCEs. Initial synthesis of 10% cross-linked elastomer doped by 2% Disperse Orange 3 (DO3) was completed at the Liquid Crystal Institute at Kent State University. Synthesis was completed as described in literature.[2,5,8,10,20]

The polymer, polymethylhydrosiloxane, was transferred by pipettor in a mass of 60 mg. DO3 was added in 4.86 mg by spatula to 238.15989 mg of the mesogen, 4-methoxyphenyl 4-(but-3-enyloxy)benzoate. The doped mesogen was then added to the polymer. The cross-linker, 1,4-bis(undec-10-enyloxy)benzene, was added to the mixture in a mass of 41.378416 mg . The mixture was dissolved in 1.0 mL thiophene free toluene. Once the mixture was dissolved, the Pt

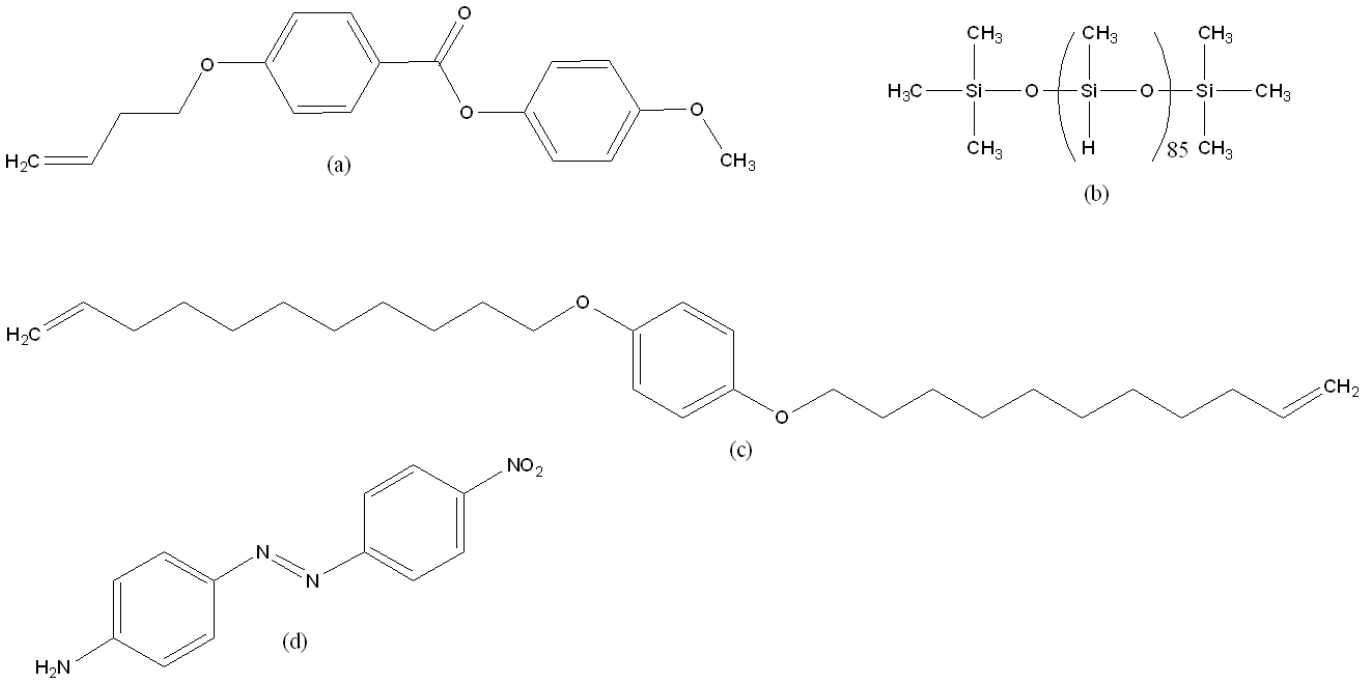

Figure 2.1. Structures of the four components of the liquid crystal elastomer used for this study. The mesogen, (a), is 4-methoxyphenyl 4-(but-3-enyloxy)benzoate. The polymer, (b), is polymethylhydrosiloxane. The cross-linker, (c), is 1,4-bis(undec-10-enyloxy)benzene. The dye, (d), is Disperse Orange 3, or (E)-4-((4-nitrophenyl)diazenyl)aniline.

catalyst was added by Hamilton syringe in 14 μL.

The spin casting apparatus (Figure 2.2) was preheated to 65°C and the above mixture was added by syringe. The spin casting apparatus was allowed to spin for approximately one hour. The spinning aligned the components of the system, allowing the cross-links to form and the liquid crystals to orient along the long axis of the elastomer. This drove the reaction to 80% completion.[20] The orientation was not yet nematic, but the elastomer took its gel-like properties in this step.

The spin casting head was removed from the apparatus following the spinning and placed in dry ice to cool to room temperature. The elastomer strip was removed from the spin casting apparatus using a razor, and Tefzel tape was used to secure the elastomer flat on a Teflon sheet. A razor was used to cut the sample into four sections, and each section was hung using the Tefzel tape. The left and right edges were also removed by razor to prevent cracking of the samples.

Paperclips were used to apply weight to the bottoms of the samples, thus stretching them

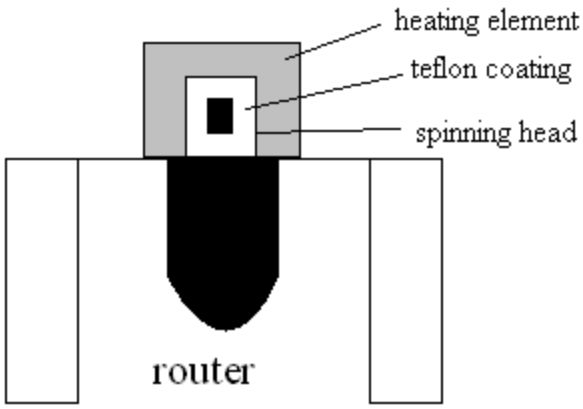

Figure 2.2. Basic schematic of spin casting apparatus. The router is mounted upside-down on the bottom of the table and is attached to the removable spinning head. The inside of the spinning head is coated with Teflon and the elastomer is held in the innermost cavity. The heating element fully encloses the spinning head.

and increasing the nematic order. Additional paper clips were added in 30-minute intervals, with the number of paperclips dictated by the stretchiness of the elastomer. Once the elastomers were sufficiently aligned, the paperclips were removed and the elastomer samples were heated at 60°C in an oven for 18 hours. Samples were stored on Teflon film to ensure they remained clean.

2.2 Finding Young's Modulus of LCEs. The determination of Young's modulus in the LCE samples is important to make a conceptual correlation between stress and birefringence of the LCEs. The process is outlined as follows.

Initial length measurements of the LCE were made without stress, which was 0.0210 m.

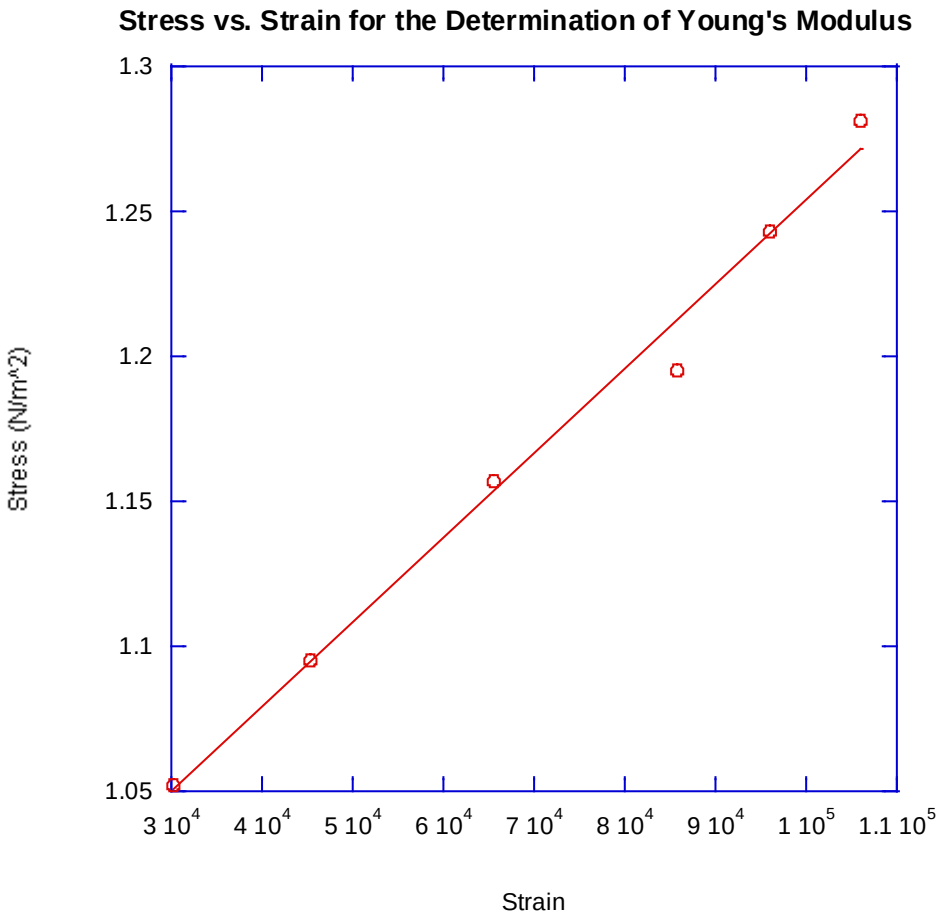

Figure 2.3. Plot of stress vs. strain for the liquid crystal elastomer with a cross-linker density of 10%. The slope of the line gave the material's Young's Modulus of $2.91 \times 10^{-6} \frac{m^2}{N}$.

The width and thickness were also measured (0.0033 m and 0.00040 m, respectively) in order to calculate the cross-sectional area, which was 1.3×10^{-6} m^2. A selection of small paperclips were massed on a balance and placed on a grid indicating each paperclip's mass. Another paperclip was cut so that only one loop remained and that loop was also massed. The loop was then taped to the free end of the elastomer, and the new length was recorded. Additional paperclips were added, tabulating the applied mass and the new length at each mass until the stretching limit was reached.

Applied forces were calculated from the masses. The forces were divided by the cross-sectional area in order to obtain the applied stress. The original length was subtracted from the new lengths, and the difference was divided by the original length in order to obtain the strain. The stress and strain were plotted linearly in KaleidaGraph 4.0 and fit with a linear trend. The slope of the trend provided the Young's modulus for the elastomer, which was $2.91 \times 10^{-6} \frac{m^2}{N}$.

2.3 Theory of PEM. In order to justify the experimental methods set forth in this study, a description of the theory behind the photoelastic modulator (PEM) must be presented. As a central apparatus in the setup, knowing exactly what the PEM does is essential.

The PEM is a useful optical instrument frequently used to measure circular and linear dichroism and optical rotation, as well as for ellipsometry, polarimetry, reflection difference spectroscopy, and FTIR double modulation. Of course, its additional ability to measure birefringence is of particular interest to us.

The PEM contains a thin quartz crystal which it stretches and contracts rapidly by a piezoelectric transducer. The applied stress causes the crystal to become birefringent through the photoelastic effect. The birefringence at any point in the oscillation is proportional to the strain in the crystal. Consequently, the PEM produces an oscillation of phase shifts. When the crystal

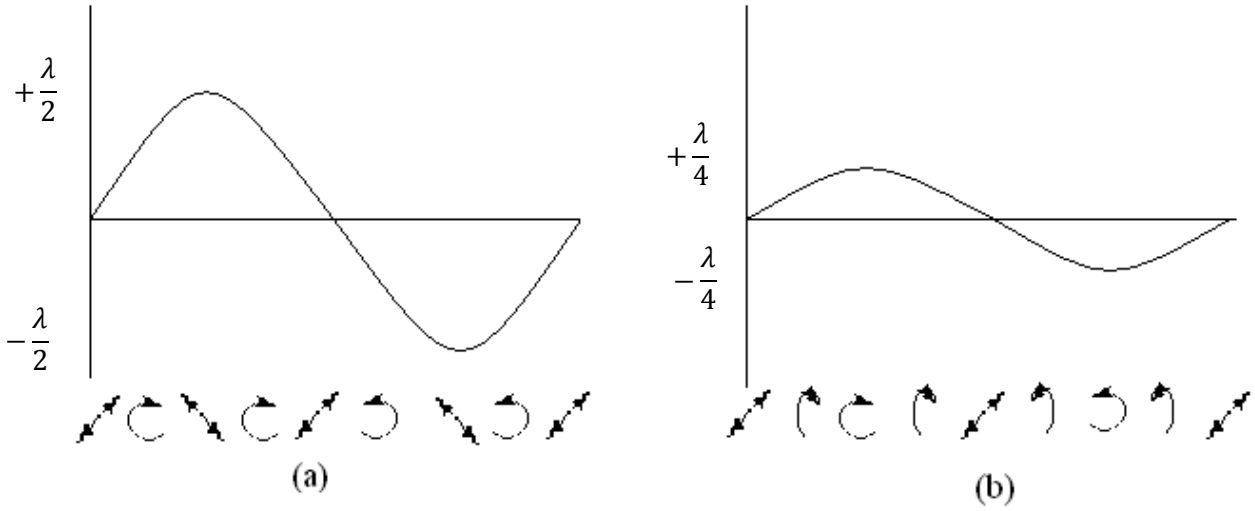

Figure 2.4. Diagram showing how waves behave after passing through a PEM at maximum retardation of (a) $\frac{\lambda}{2}$ and (b) $\frac{\lambda}{4}$.[23]

is stretched, the vertical component is faster; whenever the crystal is compressed, the horizontal component is faster. The phase shifts are called retardations.[21]

Interesting phenomena occur at half- and quarter-wave retardation. In half-wave retardation, the retardation peaks are at one half the wavelength of the incident light. As a result, 90° shifts in polarization occur, causing the light to be linearly polarized at 0, minima, and maxima retardations in orientation alternating by 90° with circular polarizations in between. The circular polarizations reverse direction at every 0 point of retardation. In quarter-wave retardation, the wave alternates between right circular polarization at the maxima and left circular polarization at the minima with linear polarization at all 0 points. In between these states, the light is elliptically polarized, switching directions around each 0 point. These phenomena are represented in Figure 2.4.[21]

Since the PEM depends on its birefringence to provide us with information, it is important to make sure the light is not polarized either completely vertically or completely

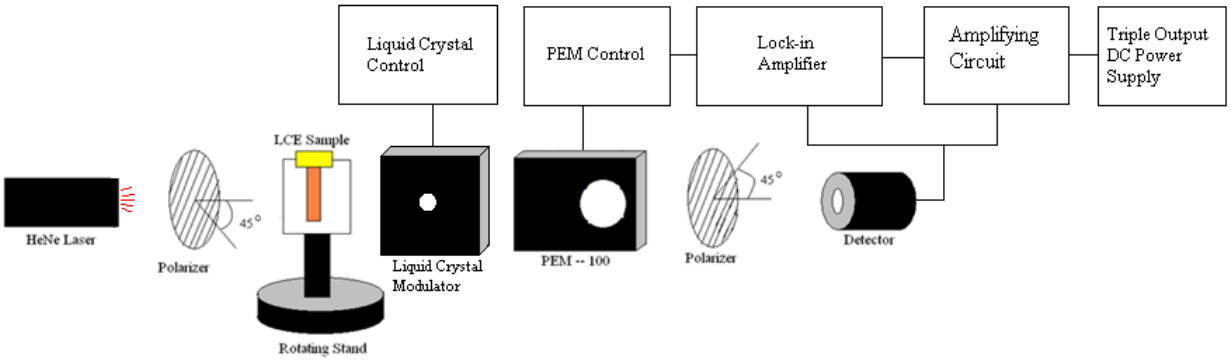

Figure 2.5. Diagram detailing experimental setup for birefringence measurements. Note that the sample was covered by a sound and temperature insulating box, and the HeNe passed through a beam expander before entering the first polarizer.

horizontally. If it is, there would only be one component of the wave, and therefore no birefringence could occur. Consequently, we use the first polarizer depicted in Figure 2.5 to give the light both x- and y-components, allowing the birefringence to occur both in the sample and in the PEM.

2.4 Measurement of Birefringence in LCEs. The experimental setup was that shown in Figure 2.5. The sample was covered with a sound– and temperature–insulating box to reduce noise effects. A Melles Griot Helium – Neon laser with a maximum output of 15 mW and a wavelength of 632.8 nm was the light source used. The PEM – 100 and detector were both produced by Hinds Instruments. The Liquid Crystal Modulator Controller was produced by Newport. The amplifying circuit was powered by a Hewlett Packard Triple Output DC Power Supply. The circuit itself is detailed in Figure 2.6. Data were collected on a Stanford Research Systems SR530 lock-in amplifier.

PEM was set to a wavelength of 632.8 nm, a retardation of 0.383 λ, and a frequency of 50.094 kHz. The laser was turned on and the apparatus aligned to ensure detection. A beam expander was used to ensure that the beam irradiated the entire sample. The amplifier's power supply was set to 2.00 V. The detector signal was split into two, one going directly into the lock-

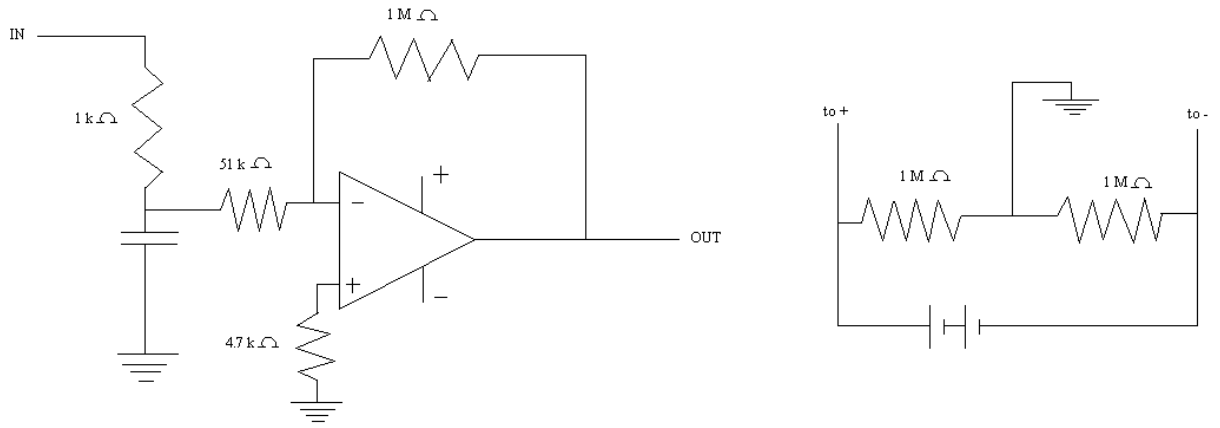

Figure 2.6. Amplifying circuit used in the setup described in Figure 2.5. The power supply was a Hewlett Packard Triple Output DC Power Supply.

in to provide the first harmonic information and the other going through the amplifier, and then into the lock-in as a denominator, thus dividing the first harmonic term by the DC term. This will prove useful in data analysis.

In order to calibrate the experiment, the sample was set normal to the laser and the liquid crystal modulator was adjusted until the signal on the lock-in reached a maximum. That maximum was recorded, and the modulator was adjusted until it reached minimum. The average of these was taken, and the signal will be divided by this number to account for the amplifier. The modulator was then adjusted until the signal was zero.

Because the sample is thick at 400 μm, there is an angle dependence in the phase shift. Consequently, the sample was rotated 2.5 degrees in both directions from normal, and data was collected at every half degree. This allowed for testing of the angle dependence while allowing the small angle approximation to remain valid during data analysis. This process was performed on the sample first with no mass suspended from the bottom, and then was repeated with each 0.3677 g and 0.4664 g suspended from the bottom of the sample using the paperclip method described in the synthesis.

2.5 Data Analysis. Having conducted the experiment and obtained the data, we must still manipulate it in order to obtain the desired birefringence data. The analysis is based on a Fourier Series expansion of the equation for the intensity of light at the detector in our setup.[21]

$$I'' = \frac{1-\cos(\Delta\phi)J_0(A_0)}{DC} + \frac{2\sin(\Delta\phi)J_1(A_0)\cos(2\Omega t)}{1f} + \frac{2\cos(\Delta\phi)J_2\cos(2\Omega t)}{2f} + \cdots \quad (2.1)$$

$\Delta\phi$ is the phase shift – which we intend to ultimately find – J_i are the Bessel functions, and A_0 is a constant we fix at 2.405 radians, the reason for which will be explained shortly. The first term is the DC term, the second is the first harmonic, and the third is the second harmonic. For our analysis, only the DC term and the first harmonic will be necessary.

From this expansion, we can isolate each the DC, and first harmonic terms. Those are given below.[21]

$$V_{DC} = K[1 - \cos(\Delta\phi)\, J_0(A_0)] \quad (2.2)$$

$$V_{1f(peak)} = 2Ksin(\Delta\phi)J_1(A_0)\cos(\Omega t) \quad (2.3)$$

K is a proportionality constant and is the same for all three terms. By setting A_0 equal to 2.405 radians, the DC term is no longer dependent on birefringence,[21] and we can thus simplify our problem. We do this by setting the retardation on the PEM to 0.383 waves, which corresponds to that radian value. Now we can use the DC term to normalize the first harmonic, simplifying them.[21]

$$\frac{V_{1f(peak)}}{V_{DC}} = 2\sin(\Delta\phi)\, J_1(A_0) \quad (2.4)$$

Since the lock-in amplifier does not return data in the form of peak values, but instead in RMS voltages, we must relate the above values to the data we receive from the lock-in by dividing by $\sqrt{2}$. The ratio, $R_{1f,}$ is thus found, and given below.[21]

$$R_{1f} = \frac{V_{1f(RMS)}}{V_{DC}} = \sqrt{2}\sin(\Delta\phi)\, J_1(A_0) \quad (2.5)$$

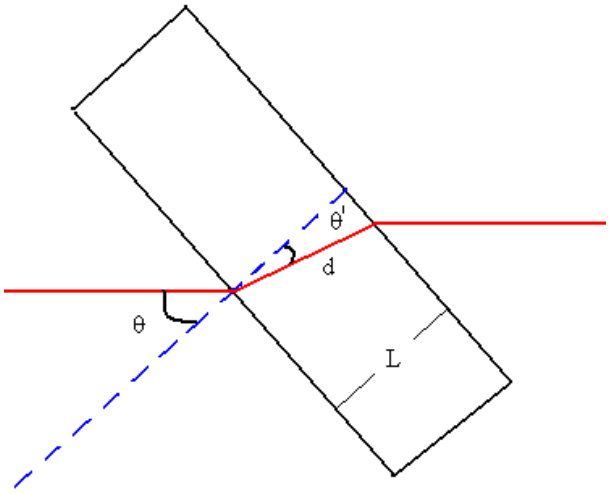

Figure 2.7. Light travelling through a thick refractive medium at an angle other than normal.

The setup performed this operation for us, as described above, so all raw data was gathered in the form of R_{1f}. Solving for $\Delta\phi$, we get our desired value in terms of constants and experimental data.[21]

$$\Delta\phi = \sin^{-1}\left[\frac{R_{1f}}{\sqrt{2}J_1(A_0)}\right] \tag{2.6}$$

Now we may recall Equation 1.12:

$$\Delta\phi = \left(\frac{2\pi}{\lambda_0}\right) d\Delta n \tag{2.7}$$

The birefringence has been rewritten as Δn here for convenience. Also note that λ_0 is the wavelength of light in air and d is the distance the light must travel through the birefringent medium. This latter term is where the angle-dependence of our study comes into play.

Consider a thick medium and light incident on that medium at some angle to the normal, as shown in Figure 2.7. The light is refracted in the material and follows a path longer than the thickness of the sample. The specific distance that it travels is contingent upon the angle the refracted light forms with the normal direction according to the definition of the cosine.

$$d = \frac{L}{\cos(\theta')} \tag{2.8}$$

In order to relate the known angle of incidence to the angle the refracted light makes with the normal, we now consider Snell's Law of Refraction for light initially in air meeting a refractive medium:

$$\sin(\theta) = n\sin(\theta') \tag{2.9}$$

Using trigonometric identities, we can now describe the path length in terms of the angle of incidence.

$$d = \frac{L}{\left[1-\frac{\sin^2(\theta)}{n^2}\right]^{\frac{1}{2}}} \tag{2.10}$$

We can expand this term by

$$d = d|_{\theta=0} + \frac{dd}{d\theta}|_{\theta=0}\theta + \frac{1}{2}\frac{d^2d}{d\theta^2}|_{\theta=0}\theta^2 \tag{2.11}$$

which simplifies to

$$d = L + \frac{L}{2n^2}\theta^2 \tag{2.12}$$

By plotting θ^2 as the *x*-value and $\Delta\phi$ as the *y*-value, we can now find the relative birefringence of our material. The slope of a linear fit to the graph would be defined as

$$m = \frac{\pi L}{\lambda_0}\frac{\Delta n}{n^2} \tag{2.13}$$

where n^2 is the square of the average birefringence along each axis. Therefore, the relative birefringence of the material is given by

$$\frac{\Delta n}{n^2} = \frac{m\lambda_0}{\pi L} \tag{2.14}$$

From the intercept, we can determine the birefringence of the elastomer. The intercept is given by

$$b = \frac{2\pi L\Delta n}{\lambda_0} \tag{2.15}$$

So the birefringence is

$$\Delta n = \frac{b\lambda_0}{2\pi L} \tag{2.16}$$

The value of n^2 can be found by

$$n^2 = \frac{b}{2m} \tag{2.17}$$

and should be on the order of 2.25.

The effect of applied stress on the birefringence of liquid crystal elastomers can be loosely analyzed by observing the trends in the data.

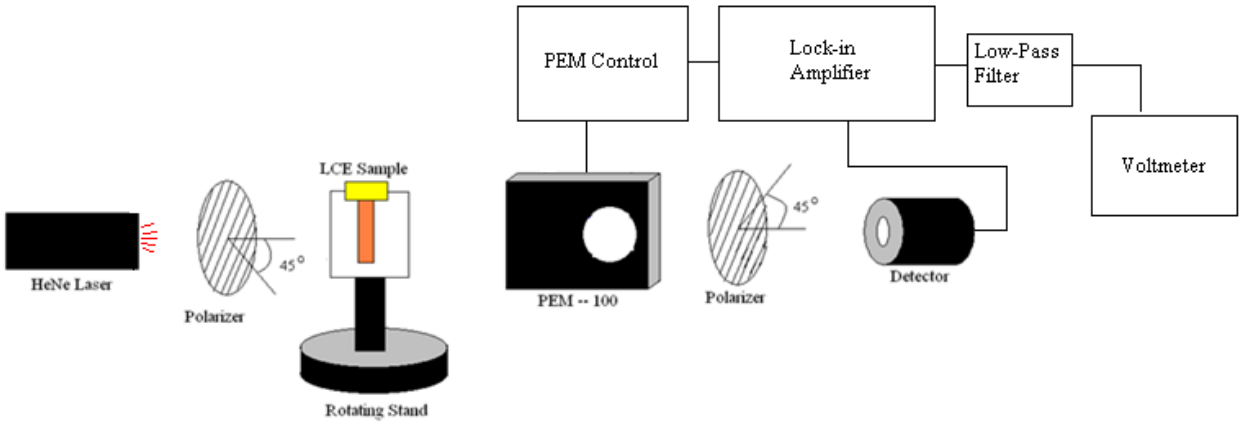

Figure 3.1. Initial experimental setup. The sample was free-hanging and the DC term was taken separately from the first harmonic term by using a voltmeter.

3. Results and Discussion. Unfortunately, the study was met with a great deal of difficulty, and those issues will be reported here. Over the span of experimentation, several adjustments were made to the methods, but never to the achievement of sensible, reproducible results. Here I will discuss each method chronologically, detailing what results the experiments produced, why those results were untrustworthy, what was postulated to be the cause of the problem, and how it was corrected for further methods.

3.1 Progression of Setups. The setup described in Figure 3.1 was the first used. The sample was initially simply hanging from the holder with no cover, and the detector went only into the lock-in amplifier, with a voltmeter connected to the lock-in in order to read the DC signal.

Data collected using this method were very noisy. In fact, it was observed early in the attempts to gather data of the elastomer with no applied stress that the signal for the first harmonic changed too drastically, frequently, and randomly to get a reading. Consequently, an attempt was made to take measurements on the sample under the stress induced by a mass of 0.4785 g in hopes that the mass would keep the sample more stationary. The results of that test were extremely scattered and the plot is shown in Figure 3.2. The phase shift values for each θ^2 value were averaged and plotted, as seen in Figure 3.2 (a), and the birefringence obtained was -2.22×10^{-4}. However, the point at zero was a graphical outlier, so it was removed from the plot, as seen

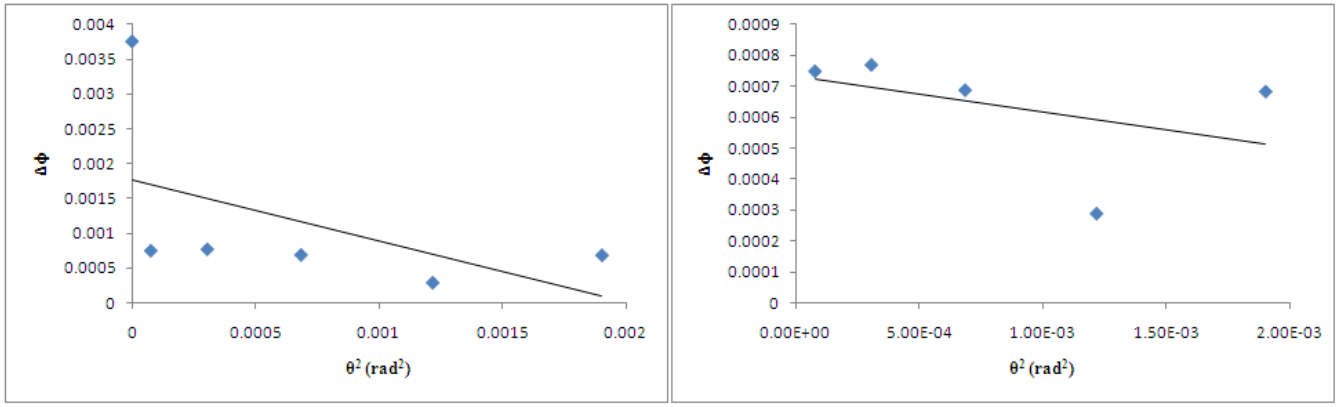

Figure 3.2. Plots of data from initial experiment, suspending a mass of 0.4785 g. (a) represents the full scope of data, and (b) represents the data after the removal of the graphical outlier at 0.

in Figure 3.2 (b). The birefringence from this graph had an absolute value an order of magnitude smaller at -2.87×10^{-5}. Future attempts at this measurement were utterly unsuccessful due to noise in the first harmonic signal, and thus reproducibility could never be confirmed.

A possible cause of noise in the measurement was the effect of vibrations on the sample, including those produced by sound and movement. A box was constructed to block out these effects and was placed over the sample during measurements. The stability of the data was tracked using LabView. The data did not stabilize, however, so in order to eliminate temperature as a consideration, foam was inserted into the inside of the box to insulate it. Experiments were conducted again, and the data remained unstable. Examples of unstable data are presented in Figure 3.3.

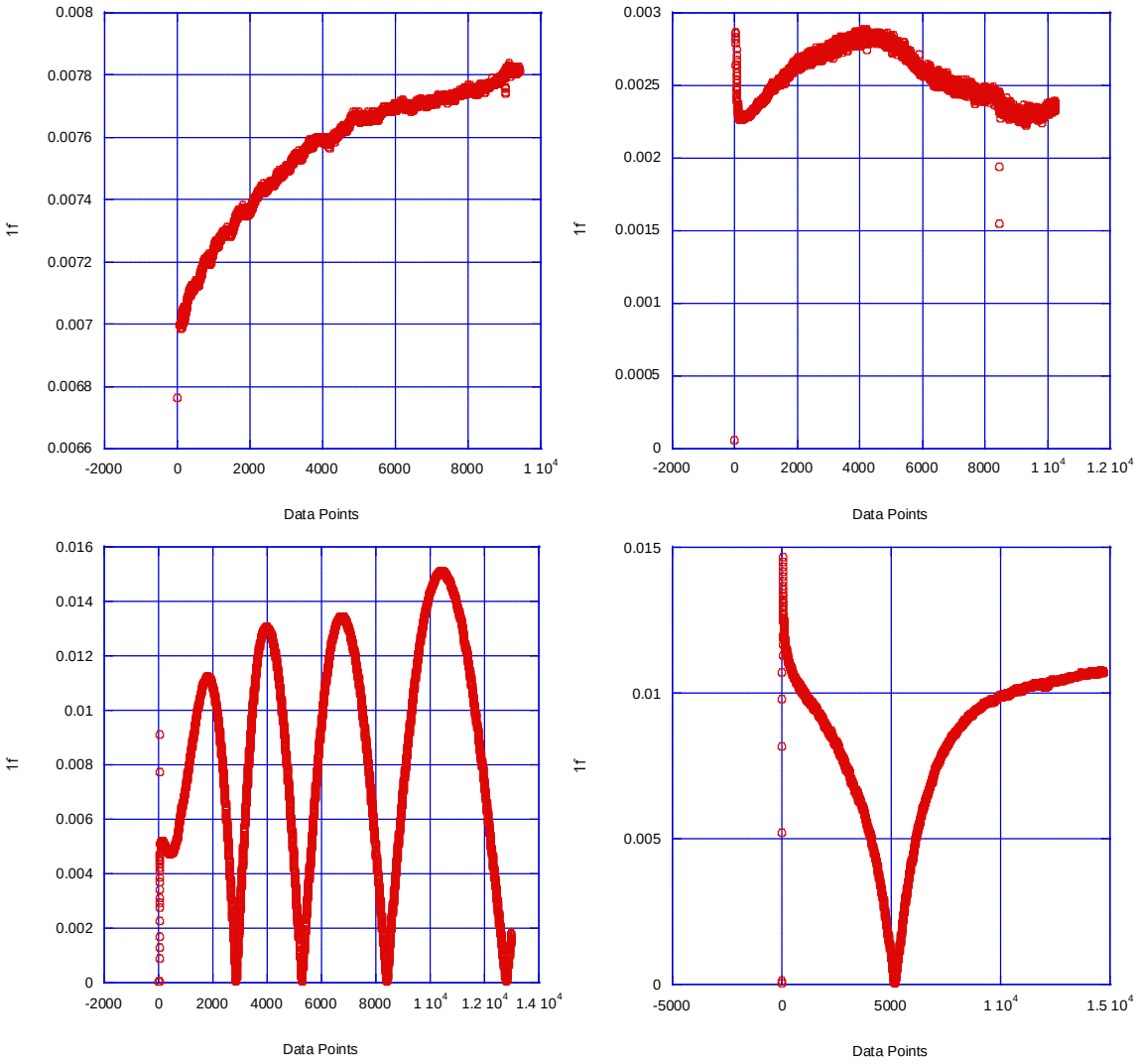

Figure 3.3. Four examples of unstable data collected on Lab View to test the effectiveness of the insulating box. The data were supposed to be essentially straight, horizontal lines across the plot, but as can be observed in all four images, the data changed significantly with time, and since all the tests were completed using the same method, the error seemed random.

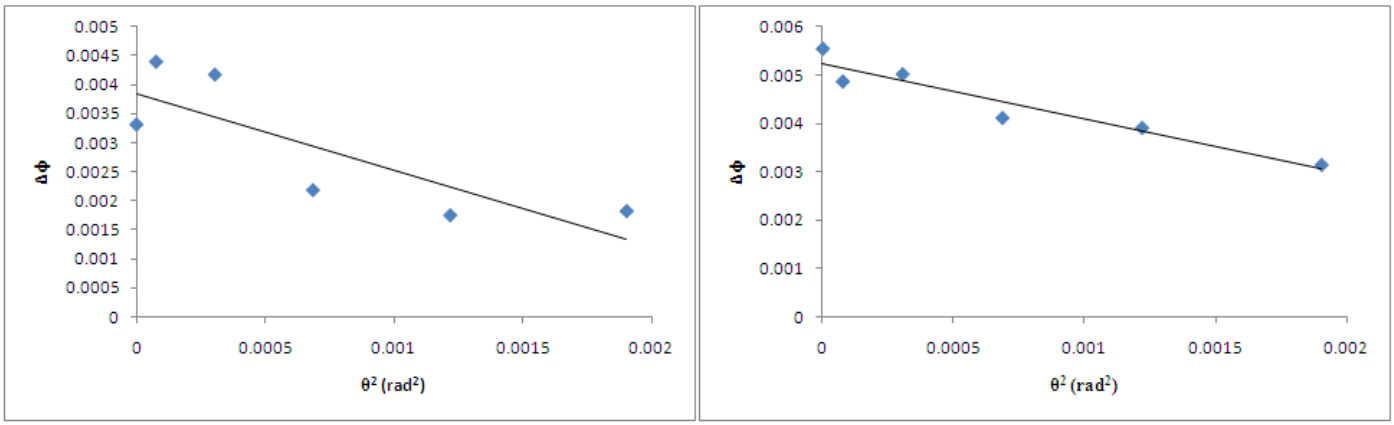

Figure 3.4. Plots of data for (a) unstressed elastomer and (2) an applied mass of 0.4464 g. The unstressed elastomer had a relative birefringence of -6.61 × 10^{-4} and the elastomer under the stress of a 0.4464 g mass had a relative birefringence of -5.71 × 10^{-4}. While these results are theoretically reasonable, there was high variance in the data that produced them, and the data was not properly calibrated, making them invalid.

It was observed, however, that the first harmonic and DC terms seemed to be changing comparably with each other, so the setup was adjusted to get the R_{1f} term directly from the lock-in by putting the DC signal through a large dynamic range amplifier and into the denominator input of the lock-in. This accomplished the goal to some degree, and data was collected again, this time for the unstressed elastomer and the condition of stress induced by 0.4464 g. The results of these tests seemed reasonable, and are presented in Figure 3.4. The unstressed relative birefringence was -6.61× 10^{-4}. For the stress 0.4464 g trial, the relative birefringence was -5.71 × 10^{-4}. These are reasonable values, and it was also reasonable that the birefringence got closer to zero when the stress was applied because the straightening of the elastomer causes and unfolding of the hairpins, and thus a disordering of the side chain liquid crystals, as show in Figure 1.7. However, there was a great deal of variance in each test for each value of θ^2, ranging to upwards of 10%, so the data were unreliable.

In order to reduce the variance, a circuit was designed to replace the large dynamic range amplifier. It is pictured in Figure 2.6, and is part of the current setup. It was powered by a

Hewlett Packard Triple Output DC Power Supply. The power supply was set to 2.00 V, and data were collected again. However, because the system was not calibrated properly for the addition of an amplifier, the results were unreliable. This was also the case for the large dynamic range amplifier, so regardless of the believability of the data, it was invalid. This brings us to the current setup.

3.2 Current Methods and Speculation on Improvements. In order to calibrate the system, a liquid crystal modulator was placed between the sample and the PEM. The process of calibration was described in section 2.4, and will not be covered again here. Before the test, the calibration was completed and entered into the Excel document being used for data analysis. Due to the lack of

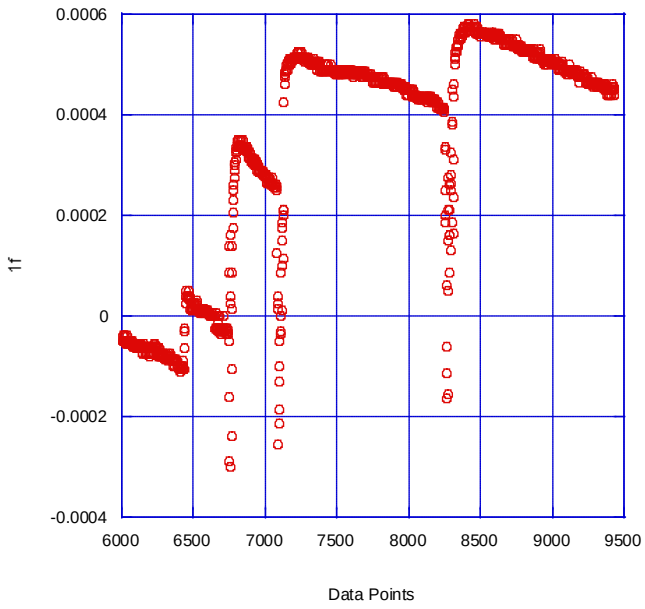

Figure 3.5. Lab View data for the most recent setup. The sudden drops in signal correspond to the process of rotating the sample. The stretches of actual data seem to have a negative linear trend. This may be the result of heating of the sample because the metal sample holder was being irradiated with the HeNe.

success with the circuit, the large dynamic range amplifier was returned to the setup, and data were collected. Unfortunately, the data were noisy and unusable again. At this point, it was speculated that the position of the laser on the sample was changing as the sample was rotated, so a beam expander was used to radiate the entire sample. The large dynamic range amplifier was then observed to be beyond its threshold on all settings, so the amplifying circuit was used again, with the power supply set to 2.00 V.

Once again, however, the data would not stabilize, and instead decreased linearly over time, as show in Figure 3.5. It seems reasonable that the decrease in the signal is due to an increase in the temperature of the sample, since increased temperature results in decreased order, and thus decreased birefringence, as discussed in Section1. Due to the beam expander, the entire elastomer and the metal sample holder were all being irradiated, and since metal conducts heat, it may be warming up the sample steadily throughout the test. Consequently, the next step in solving the problems in methodology is to design a sample holder that will not conduct heat.

4. Conclusions. Since the methods did not return reliable results, no conclusions can be made about the dependence of birefringence in elastomers on the stress applied to them; however, through the repeated difficulties, a great deal has been learned about the experimentation itself, and hopefully that new knowledge will propel future researchers to success in these tests. The experiment and setup were repeatedly adjusted to no avail, but each adjustment did improve the setup in some way, and the experiments are closer to success now than they were in September.

Further tests with new adjustments will be completed in the coming weeks in an effort to at least establish a working procedure for a future student to complete this project, if not to gather sufficient data to come to some conclusion about the system.

5. Future Considerations. Once the problems with the experiment are corrected, and data are collected on the experiment proposed in this study, a series of directions could be taken. One option is varying the cross-linker density and measuring the effects on the Young's Modulus of the material and then on the birefringence under stress. Another would be to study the differences between main chain elastomers and side chain elastomers, analyzing how the structure differences contribute to the birefringence.

If the appropriate apparatus could be constructed, it would also be interesting to observe the effects of irradiating the elastomer with a blue laser and studying the effects of the dye isomerization on the birefringence of the material. The difficulty with this experiment is that blue lasers cause elastomers to bend, so the angle-dependent phase shift would be difficult to measure without first finding some way to hold the elastomer perfectly in place.

Of course, none of these experiments are possible without first solving the last few problems with the experimental setup, so the most immediate future consideration is doing just that.

Appendix A: Complete Tabulation of Raw Data.

Elastomer suspending 0.4785 g, initial experiment.

theta	theta rad	1f	DC	DC mV	R1f	theta^2	delta phi
0	0	0.27	0.054	54	0.005	0	0.006811
0	0	-0.115	-0.22	-220	0.000523	0	0.000712
-0.5	-0.00873	-0.027	-0.048	-48	0.000563	7.62E-05	0.000766
-0.5	-0.00873	0.06	0.114	114	0.000526	7.62E-05	0.000717
0.5	0.008727	-0.01	-0.017	-17	0.000588	7.62E-05	0.000801
0.5	0.008727	0.04	0.077	77	0.000519	7.62E-05	0.000708
-1	-0.01745	-0.027	-0.053	-53	0.000509	0.000305	0.000694
-1	-0.01745	-0.018	-0.025	-25	0.00072	0.000305	0.000981
1	0.017453	0.07	0.138	138	0.000507	0.000305	0.000691
1	0.017453	0.013	0.025	25	0.00052	0.000305	0.000708
-1.5	-0.02618	0.046	0.093	93	0.000495	0.000685	0.000674
-1.5	-0.02618	-0.052	-0.097	-97	0.000536	0.000685	0.00073
1.5	0.02618	0.019	0.044	44	0.000432	0.000685	0.000588
1.5	0.02618	-0.046	-0.083	-83	0.000554	0.000685	0.000755
-2	-0.03491	0.04	0.078	78	0.000513	0.001218	0.000699
-2	-0.03491	0.045	-0.085	-85	-0.00053	0.001218	-0.00072
2	0.034907	0.036	0.075	75	0.00048	0.001218	0.000654
2	0.034907	0.021	0.055	55	0.000382	0.001218	0.00052
-2.5	-0.04363	-0.106	-0.208	-208	0.00051	0.001904	0.000694
-2.5	-0.04363	-0.103	-0.199	-199	0.000518	0.001904	0.000705
2.5	0.043633	0.065	0.146	146	0.000445	0.001904	0.000606
2.5	0.043633	0.077	0.145	145	0.000531	0.001904	0.000723

Unstressed elastomer, setup with no LC modulator, and using the large dynamic range amplifier.

theta	theta rad	R1f	Sens Adj	theta^2	delta phi
-2.5	-0.04363	3.06	0.00306	0.001903859	0.004168
-2.5	-0.04363	2.66	0.00266	0.001903859	0.003623
-2.5	-0.04363	2.03	0.00203	0.001903859	0.002765
-2.5	-0.04363	3.71	0.00371	0.001903859	0.005054
-2.5	-0.04363	3.99	0.00399	0.001903859	0.005435
-2.5	-0.04363	0.06	0.00006	0.001903859	8.17E-05
-2	-0.03491	3.04	0.00304	0.00121847	0.004141
-2	-0.03491	3.19	0.00319	0.00121847	0.004345
-2	-0.03491	0.76	0.00076	0.00121847	0.001035
-2	-0.03491	3.5	0.0035	0.00121847	0.004768
-2	-0.03491	0.56	0.00056	0.00121847	0.000763
-2	-0.03491	0.52	0.00052	0.00121847	0.000708
-1.5	-0.02618	3.54	0.00354	0.000685389	0.004822
-1.5	-0.02618	2.28	0.00228	0.000685389	0.003106
-1.5	-0.02618	0.06	0.00006	0.000685389	8.17E-05
-1.5	-0.02618	2.69	0.00269	0.000685389	0.003664
-1.5	-0.02618	0.07	0.00007	0.000685389	9.54E-05
-1.5	-0.02618	0.18	0.00018	0.000685389	0.000245
-1	-0.01745	3.52	0.00352	0.000304617	0.004795
-1	-0.01745	3.5	0.0035	0.000304617	0.004768
-1	-0.01745	3.15	0.00315	0.000304617	0.004291
-1	-0.01745	2.23	0.00223	0.000304617	0.003038
-1	-0.01745	0.2	0.0002	0.000304617	0.000272
-1	-0.01745	4.15	0.00415	0.000304617	0.005653
-0.5	-0.00873	3.11	0.00311	7.61544E-05	0.004236
-0.5	-0.00873	3.01	0.00301	7.61544E-05	0.0041
-0.5	-0.00873	3.95	0.00395	7.61544E-05	0.005381
-0.5	-0.00873	2.98	0.00298	7.61544E-05	0.004059
-0.5	-0.00873	2.04	0.00204	7.61544E-05	0.002779
-0.5	-0.00873	3.23	0.00323	7.61544E-05	0.0044
0	0	3.4	0.0034	0	0.004631
0	0	4.61	0.00461	0	0.00628
0	0	2.09	0.00209	0	0.002847
0	0	2.03	0.00203	0	0.002765
0	0	0.25	0.00025	0	0.000341
0	0	2.18	0.00218	0	0.002969
0.5	0.008727	3.62	0.00362	7.61544E-05	0.004931
0.5	0.008727	4.13	0.00413	7.61544E-05	0.005626

0.5	0.008727	0.76	0.00076	7.61544E-05	0.001035
0.5	0.008727	4.05	0.00405	7.61544E-05	0.005517
0.5	0.008727	3.28	0.00328	7.61544E-05	0.004468
0.5	0.008727	4.79	0.00479	7.61544E-05	0.006525
1	0.017453	2.31	0.00231	0.000304617	0.003147
1	0.017453	2.46	0.00246	0.000304617	0.003351
1	0.017453	4.49	0.00449	0.000304617	0.006116
1	0.017453	4.05	0.00405	0.000304617	0.005517
1	0.017453	1.39	0.00139	0.000304617	0.001893
1	0.017453	5.25	0.00525	0.000304617	0.007151
1.5	0.02618	0.73	0.00073	0.000685389	0.000994
1.5	0.02618	0.86	0.00086	0.000685389	0.001171
1.5	0.02618	2.57	0.00257	0.000685389	0.003501
1.5	0.02618	2.46	0.00246	0.000685389	0.003351
1.5	0.02618	0.07	0.00007	0.000685389	9.54E-05
1.5	0.02618	3.65	0.00365	0.000685389	0.004972
2	0.034907	0.08	0.00008	0.00121847	0.000109
2	0.034907	0.13	0.00013	0.00121847	0.000177
2	0.034907	0.4	0.0004	0.00121847	0.000545
2	0.034907	0.83	0.00083	0.00121847	0.001131
2	0.034907	1.05	0.00105	0.00121847	0.00143
2	0.034907	1.27	0.00127	0.00121847	0.00173
2.5	0.043633	0.12	0.00012	0.001903859	0.000163
2.5	0.043633	0.1	0.0001	0.001903859	0.000136
2.5	0.043633	0.05	0.00005	0.001903859	6.81E-05
2.5	0.043633	0.05	0.00005	0.001903859	6.81E-05
2.5	0.043633	0.06	0.00006	0.001903859	8.17E-05
2.5	0.043633	0.07	0.00007	0.001903859	9.54E-05

Unstressed elastomer, no LC modulator, amplifying circuit.

theta	theta rad	R1f	Sens Adj	theta^2	delta phi
-2.5	-0.04363	-0.14	-0.00014	0.001904	-0.00019
-2	-0.03491	0.08	0.00008	0.001218	0.000109
-1.5	-0.02618	-0.21	-0.00021	0.000685	-0.00029
-1	-0.01745	-0.19	-0.00019	0.000305	-0.00026
-0.5	-0.00873	-0.73	-0.00073	7.62E-05	-0.00099
0	0	-0.72	-0.00072	0	-0.00098
0.5	0.008727	-0.57	-0.00057	7.62E-05	-0.00078
1	0.017453	-0.22	-0.00022	0.000305	-0.0003
1.5	0.02618	-0.82	-0.00082	0.000685	-0.00112
2	0.034907	-0.34	-0.00034	0.001218	-0.00046
2.5	0.043633	-0.03	-0.00003	0.001904	-4.1E-05
2.5	0.043633	-0.07	-0.00007	0.001904	-9.5E-05
2	0.034907	-0.34	-0.00034	0.001218	-0.00046
1.5	0.02618	-0.87	-0.00087	0.000685	-0.00119
1	0.017453	-0.48	-0.00048	0.000305	-0.00065
0.5	0.008727	-0.28	-0.00028	7.62E-05	-0.00038
0	0	-0.06	-0.00006	0	-8.2E-05
-0.5	-0.00873	-0.34	-0.00034	7.62E-05	-0.00046
-1	-0.01745	0.26	0.00026	0.000305	0.000354
-1.5	-0.02618	0.35	0.00035	0.000685	0.000477
-2	-0.03491	-0.13	-0.00013	0.001218	-0.00018
-2.5	-0.04363	0	0	0.001904	0
-2.5	-0.04363	0.09	0.00009	0.001904	0.000123
-2	-0.03491	0.11	0.00011	0.001218	0.00015

-1.5	-0.02618	-0.21	-0.00021	0.000685	-0.00029
-1	-0.01745	-0.16	-0.00016	0.000305	-0.00022
-0.5	-0.00873	0.55	0.00055	7.62E-05	0.000749
0	0	-0.07	-0.00007	0	-9.5E-05
0.5	0.008727	-0.38	-0.00038	7.62E-05	-0.00052
1	0.017453	-0.07	-0.00007	0.000305	-9.5E-05
1.5	0.02618	-0.43	-0.00043	0.000685	-0.00059
2	0.034907	-0.4	-0.0004	0.001218	-0.00054
2.5	0.043633	-0.14	-0.00014	0.001904	-0.00019
2.5	0.043633	-0.16	-0.00016	0.001904	-0.00022
2	0.034907	-0.5	-0.0005	0.001218	-0.00068
1.5	0.02618	-0.43	-0.00043	0.000685	-0.00059
1	0.017453	0.19	0.00019	0.000305	0.000259
0.5	0.008727	0.15	0.00015	7.62E-05	0.000204
0	0	0.23	0.00023	0	0.000313
-0.5	-0.00873	0.63	0.00063	7.62E-05	0.000858
-1	-0.01745	0.29	0.00029	0.000305	0.000395
-1.5	-0.02618	-0.15	-0.00015	0.000685	-0.0002
-2	-0.03491	-0.07	-0.00007	0.001218	-9.5E-05
-2.5	-0.04363	0.34	0.00034	0.001904	0.000463

Elastomer suspending 0.4464 g, no LC modulator and using large dynamic range amplifier

theta	theta rad	R1f	Sens Adj	theta^2	delta phi
-2.5	-0.04363	6.88	0.00688	0.001904	0.009372
-2	-0.03491	4.25	0.00425	0.001218	0.005789
-1.5	-0.02618	2.61	0.00261	0.000685	0.003555
-1	-0.01745	4.94	0.00494	0.000305	0.006729
-0.5	-0.00873	1.91	0.00191	7.62E-05	0.002602
0	0	1.5	0.0015	0	0.002043
0.5	0.008727	0.33	0.00033	7.62E-05	0.00045
1	0.017453	3.41	0.00341	0.000305	0.004645
1.5	0.02618	1.03	0.00103	0.000685	0.001403
2	0.034907	1.2	0.0012	0.001218	0.001635
2.5	0.043633	0.11	0.00011	0.001904	0.00015
2.5	0.043633	0.84	0.00084	0.001904	0.001144
2	0.034907	1.78	0.00178	0.001218	0.002425
1.5	0.02618	2.73	0.00273	0.000685	0.003719
1	0.017453	2.8	0.0028	0.000305	0.003814
0.5	0.008727	2.76	0.00276	7.62E-05	0.00376
0	0	4.08	0.00408	0	0.005558
-0.5	-0.00873	4.43	0.00443	7.62E-05	0.006034
-1	-0.01745	3.4	0.0034	0.000305	0.004631
-1.5	-0.02618	4	0.004	0.000685	0.005449
-2	-0.03491	4.21	0.00421	0.001218	0.005735
-2.5	-0.04363	4.4	0.0044	0.001904	0.005994

-2.5	-0.04363	4.94	0.00494	0.001904	0.006729
-2	-0.03491	5.34	0.00534	0.001218	0.007274
-1.5	-0.02618	3.31	0.00331	0.000685	0.004509
-1	-0.01745	2.35	0.00235	0.000305	0.003201
-0.5	-0.00873	7.16	0.00716	7.62E-05	0.009753
0	0	8.02	0.00802	0	0.010925
0.5	0.008727	2.79	0.00279	7.62E-05	0.0038
1	0.017453	4.37	0.00437	0.000305	0.005953
1.5	0.02618	4.03	0.00403	0.000685	0.00549
2	0.034907	1.62	0.00162	0.001218	0.002207
2.5	0.043633	0.43	0.00043	0.001904	0.000586
2.5	0.043633	0.45	0.00045	0.001904	0.000613
2	0.034907	1.79	0.00179	0.001218	0.002438
1.5	0.02618	4.19	0.00419	0.000685	0.005707
1	0.017453	6.53	0.00653	0.000305	0.008895
0.5	0.008727	6.24	0.00624	7.62E-05	0.0085
0	0	5.85	0.00585	0	0.007969
-0.5	-0.00873	6.46	0.00646	7.62E-05	0.0088
-1	-0.01745	3.21	0.00321	0.000305	0.004373
-1.5	-0.02618	2.36	0.00236	0.000685	0.003215
-2	-0.03491	4.19	0.00419	0.001218	0.005707
-2.5	-0.04363	2.92	0.00292	0.001904	0.003977
-2.5	-0.04363	3.64	0.00364	0.001904	0.004958
-2	-0.03491	4.9	0.0049	0.001218	0.006675

-1.5	-0.02618	3.4	0.0034	0.000685	0.004631
-1	-0.01745	2.35	0.00235	0.000305	0.003201
-0.5	-0.00873	4.55	0.00455	7.62E-05	0.006198
0	0	3.75	0.00375	0	0.005108
0.5	0.008727	1.58	0.00158	7.62E-05	0.002152
1	0.017453	2	0.002	0.000305	0.002724
1.5	0.02618	3.93	0.00393	0.000685	0.005353
2	0.034907	1.66	0.00166	0.001218	0.002261
2.5	0.043633	0.29	0.00029	0.001904	0.000395
2.5	0.043633	0.32	0.00032	0.001904	0.000436
2	0.034907	2.38	0.00238	0.001218	0.003242
1.5	0.02618	3.94	0.00394	0.000685	0.005367
1	0.017453	5.26	0.00526	0.000305	0.007165
0.5	0.008727	4.53	0.00453	7.62E-05	0.006171
0	0	1.26	0.00126	0	0.001716
-0.5	-0.00873	0.17	0.00017	7.62E-05	0.000232
-1	-0.01745	3.65	0.00365	0.000305	0.004972
-1.5	-0.02618	0.7	0.0007	0.000685	0.000954
-2	-0.03491	1.08	0.00108	0.001218	0.001471
-2.5	-0.04363	2.41	0.00241	0.001904	0.003283

Elastomer suspending 0.3677 g, no LC modulator, using large dynamic range amplifier

theta	theta rad	R1f	Sens Adj	theta^2	delta phi
-2.5	-0.04363	0.34	0.00034	0.001904	0.000463
-2	-0.03491	0.28	0.00028	0.001218	0.000381
-1.5	-0.02618	0.49	0.00049	0.000685	0.000667
-1	-0.01745	0.65	0.00065	0.000305	0.000885
-0.5	-0.00873	0.54	0.00054	7.62E-05	0.000736
0	0	0.41	0.00041	0	0.000558
0.5	0.008727	0.86	0.00086	7.62E-05	0.001171
1	0.017453	0.74	0.00074	0.000305	0.001008
1.5	0.02618	0.85	0.00085	0.000685	0.001158
2	0.034907	0.83	0.00083	0.001218	0.001131
2.5	0.043633	0.24	0.00024	0.001904	0.000327
2.5	0.043633	0.19	0.00019	0.001904	0.000259
2	0.034907	0.84	0.00084	0.001218	0.001144
1.5	0.02618	0.69	0.00069	0.000685	0.00094
1	0.017453	0.45	0.00045	0.000305	0.000613
0.5	0.008727	0.56	0.00056	7.62E-05	0.000763
0	0	0.27	0.00027	0	0.000368
-0.5	-0.00873	0.51	0.00051	7.62E-05	0.000695
-1	-0.01745	0.48	0.00048	0.000305	0.000654
-1.5	-0.02618	0.31	0.00031	0.000685	0.000422
-2	-0.03491	0.07	0.00007	0.001218	9.54E-05
-2.5	-0.04363	0.18	0.00018	0.001904	0.000245

-2.5	-0.04363	0.21	0.00021	0.001904	0.000286
-2	-0.03491	0.25	0.00025	0.001218	0.000341
-1.5	-0.02618	0.25	0.00025	0.000685	0.000341
-1	-0.01745	0.43	0.00043	0.000305	0.000586
-0.5	-0.00873	0.28	0.00028	7.62E-05	0.000381
0	0	0.5	0.0005	0	0.000681
0.5	0.008727	0.29	0.00029	7.62E-05	0.000395
1	0.017453	0.62	0.00062	0.000305	0.000845
1.5	0.02618	0.62	0.00062	0.000685	0.000845
2	0.034907	0.25	0.00025	0.001218	0.000341
2.5	0.043633	0.49	0.00049	0.001904	0.000667
2.5	0.043633	0.62	0.00062	0.001904	0.000845
2	0.034907	0.76	0.00076	0.001218	0.001035
1.5	0.02618	0.34	0.00034	0.000685	0.000463
1	0.017453	0.26	0.00026	0.000305	0.000354
0.5	0.008727	0.3	0.0003	7.62E-05	0.000409
0	0	0.39	0.00039	0	0.000531
-0.5	-0.00873	0.18	0.00018	7.62E-05	0.000245
-1	-0.01745	-0.14	-0.00014	0.000305	-0.00019
-1.5	-0.02618	0.22	0.00022	0.000685	0.0003
-2	-0.03491	0.1	0.0001	0.001218	0.000136
-2.5	-0.04363	0.17	0.00017	0.001904	0.000232

Appendix B: Photographs of Lab.



Overview of the Statman lab.

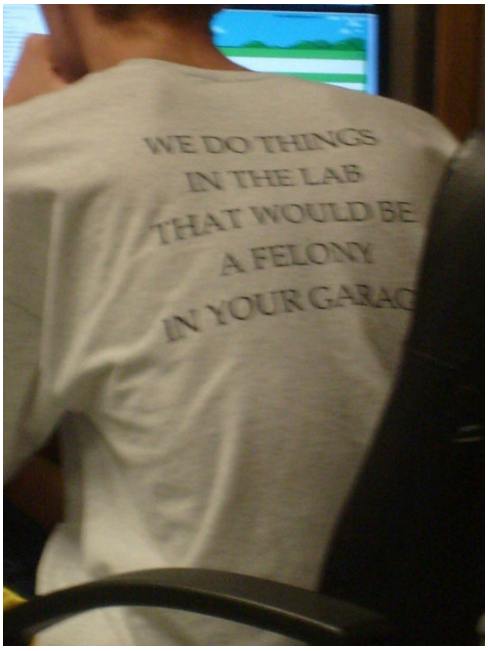

It's kind of true…



My initial setup.

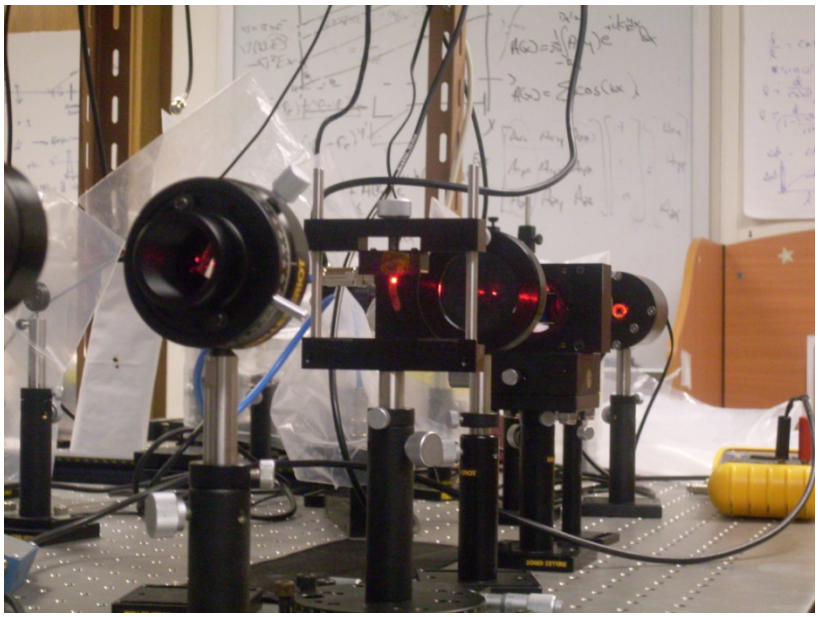

The initial setup in action.

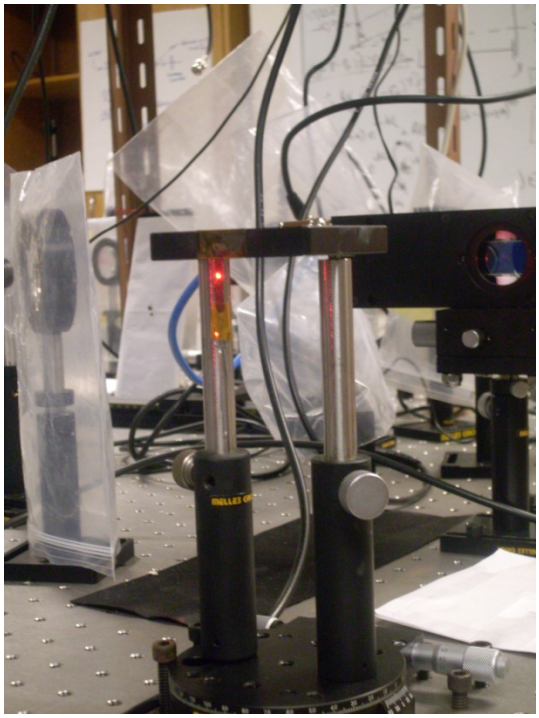

The sample being irradiated with the laser.

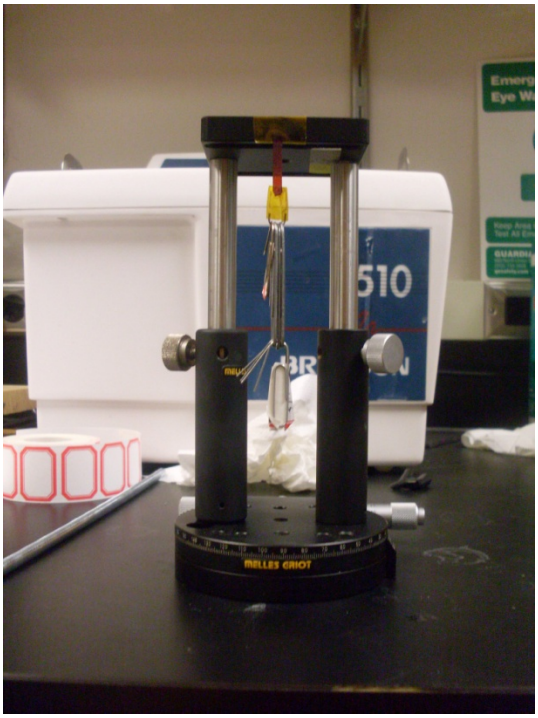

Measuring Young's Modulus

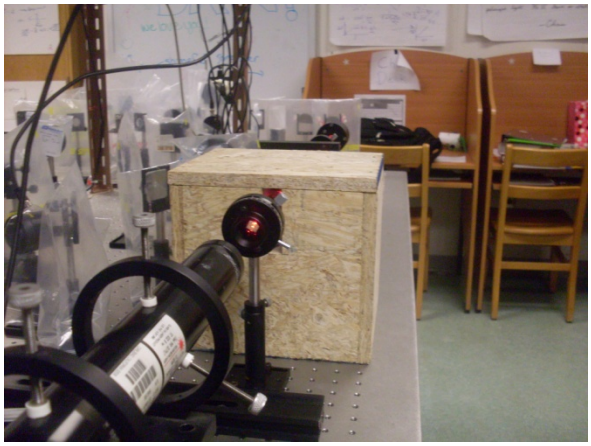

Setup with the insulating box in its infancy.



Spin caster head, top view.



Spin caster head, bottom view.



Setup with finished insulating box.

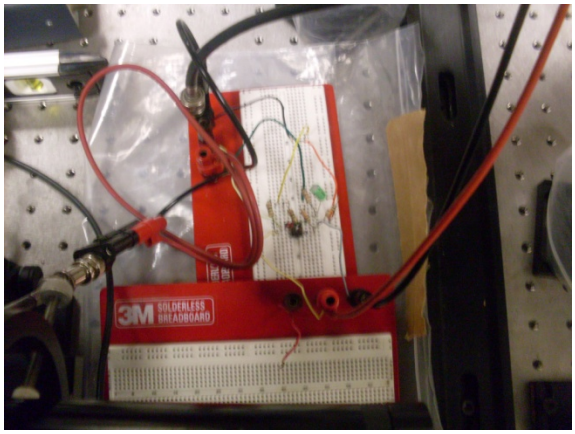

Amplifying circuit.

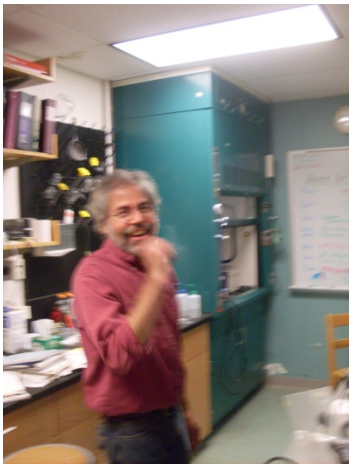

Dr. Statman is too fast for the camera.

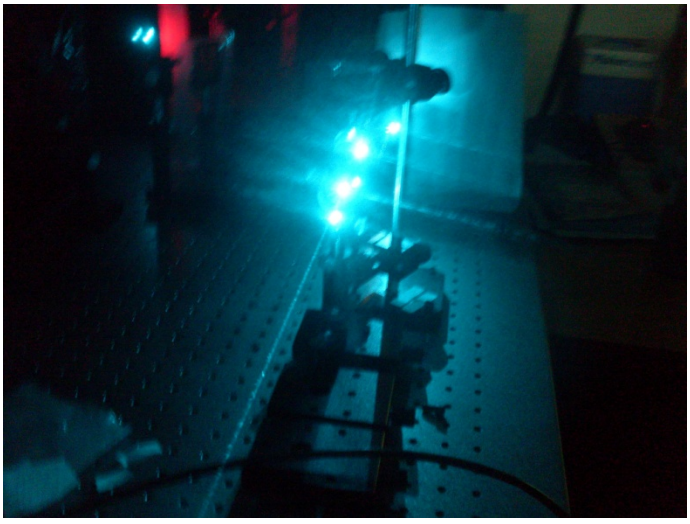

Not my setup, but it's still cool to see a laser beam.

References.

[1] Warner, M., Terentjev, E. M. *Liquid Crystal Elastomers* Revised Edition. Oxford Science Publications 2003, 2007.

[2] Xie, Ping and Zhang, Rongben. Liquid crystal elastomers, networks and gels: advanced smart materials. Journal of Materials Chemistry, 2005.

[3] Serak, Svetlana V. et al. Azobenzene liquid crystal polymer-based membrane and cantilever optical systems. Opctics Express Vol. 17, No. 18, August 31, 2009.

[4] Hrozhyk, Uladzimir et al. Bidirectional Photoresponse of Surface Pretreated Azobenzene Liquid Crystal Polymer Networks. Optics Express Vol. 17, No. 2, January 19, 2009.

[5] Camacho-Lopez, Miguel et al. Fast liquid-crystal elastomer swims into the dark. Nature Materials Vol. 3, May 2004.

[6] Corbett, D. and Warner, M. Nonlinear Photoresponse of Disordered Elastomers. The American Physical Society: Physical Review Letters, 2006.

[7] Ennis, R. et al. Nonlocal model for nematic liquid-crystal elastomers. The American Physical Society: Physical Review E, 2006.

[8] Sanchéz-Ferrer, Antoni and Finkelmann, Heino. Thermal and mechanical properties of new Main-Chain Liquid-Crystalline Elastomers. Solid State Sci. (2010), doi: 10.1016/j.solidstatesciences.2010.01.017

[9] Tokita, M. et al. Thermally Reversible Distortion Observed for Monodomain Nematic Elastomer of Cross-Linked Main-Chain Polyester. Taylor and Francis Group: Journal of Molecular and Liquid Crystals, Vol. 465, pp. 193-202, 2007.

[10] Barnes, N. R., Davis, F. J. and Mitchell, G. R. Molecular Switching in Liquid Crystal Elastomers. Journal of Molecular and Liquid Crystals, Vol. 168, pp. 13-25, 1989.

[11] Collings, Peter J. and Hird, Michael. *Introduction to Liquid Crystals: Chemistry and Physics*. Taylor and Francis Ltd. 1997.

[12] Khoo, Iam Choon. Nonlinear optics of liquid crystalline materials. Physics Reports, 2009.

[13] Wu, Shin-Tson. Birefringence dispersions of liquid crystals. The American Physical Society: Physical Review A, Vol. 33, No. 2, February 1986.

[14] Chemistry 445 Lecture

[15] Personal Communication with Dr. David Statman

[16] Desimpel, Chris. “Why Are Liquid Crystals So Interesting?” Universteit Gent Liquid Crystals and Photonics Group. http://lcp.elis.ugent.be/tutorials/lc/lc2.

[17] Feynmann, Richard P., Leighton, Robert B. and Sands, Matthew. *The Feynmann Lectures on Physics, Vol. II.* Addison Wesley Publishing Company, 1964.

[18] Pedrotti, S.J. Frank L., Pedrotti, Leno S. and Pedrotti, Leno M. *Introduction to Optics* Third Edition. Pearson Education, Inc. 2007.

[19] Hecht, Eugene. *Optics* Fourth Edition. Peason Education, Inc. pulishing as Addison Wesley, 2002.

[20] Personal Communication with Paul Luchette at Kent State University.

[21] *PEM-90 Photoelastic ModulatorSystems User Manual.* Hinds Instruments, Inc., 1998.

[22] Levinson, Joshua. Examining the Bending of Liquid Crystal Elastomers: Measuring the Dependence of Bending Angle on Liquid Crystal Reorientation and the Efficiency of Energy Transfer between Optical and Mechanical Energy. Allgheny College, 2010.

[23] Statman, David and Lombardi, Sr., James, C. Modeling the Dynamics of Photo-induced Reorientation of Nematic Liquid Crystals doped with Azo-dye. Taylor and Francis Group: Journal of Molecular and Liquid Crystals, Vol. 494, pp. 1-10, 2008.

[24] Bassotti, Elisa et al. Effect of Strain on the Photoisomerization and Stability of a Congested Azobenzenophane: A Combined Experimenal and Computational Study. Journal of Physical Chemistry A, 2006,

[25] Barrett, C., Natansohn, A. and Rochon, P. Cis-Trans Thermal Isomerization Rates of Bound and Doped Azobenzenes in a Series of Polymers. Chem. Mater., 1995.

[26] Leyssner, Felix et al. Photoisomerization Ability of Molecular Switches Adsrobed on Au(111): Comparison between Azobenzene and Stilbene Derivatives. Journal of Physical Chemistry C, 2010.

[27] Camorani, P. et al. Comparitive Study of Photomechanical Effects in Linear and Star Azo-Polymers. Taylor and Francis Group: Journal of Molecular and Liquid Crystals Vol. 500, pp. 1-9, 2009.